Modular Spacecraft with Integrated Structural Electrodynamic Propulsion

Nestor R. Voronka, Robert P. Hoyt, Jeff Slostad,
Brian E. Gilchrist (UMich/EDA), Keith Fuhrhop (UMich)

TETHERS UNLIMITED, INC.
11807 N. Creek Pkwy S., Suite B-102
Bothell, WA 98011

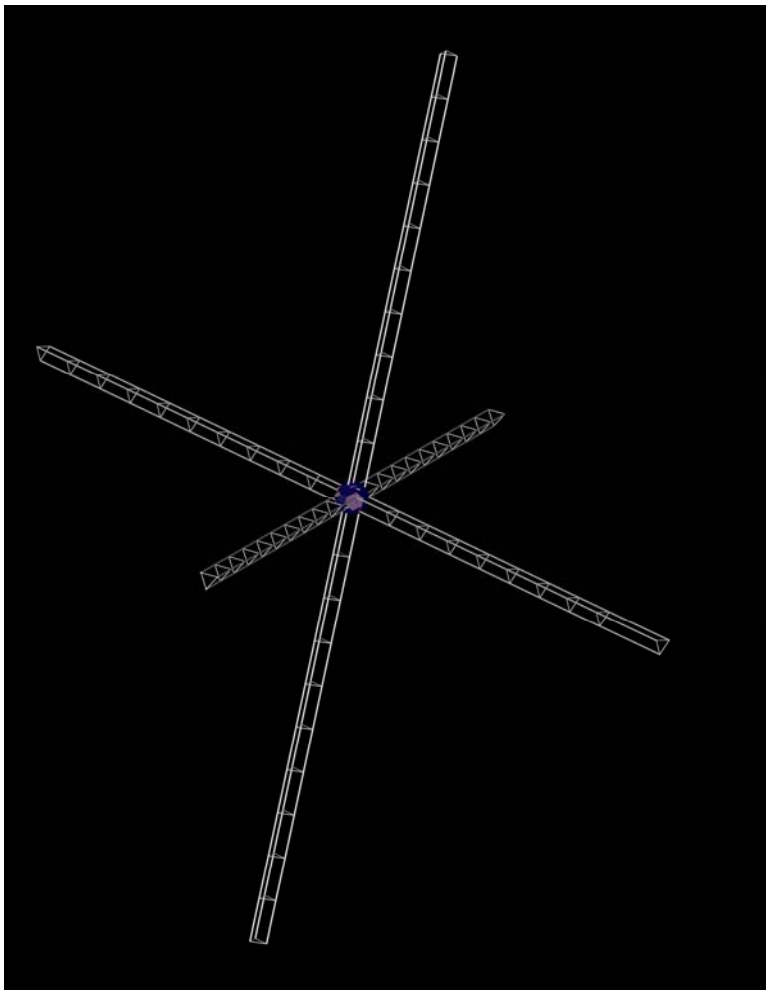

Period of Performance:
1 September 2005 through
30 April 2006

Report Date:
1 May 2006
Phase I Final Report

Contract: NAS5-03110
Subaward: 07605-003-050

Prepared for:

NASA Institute for Advanced Concepts
Universities Space Research Association
Atlanta, GA 30308

TABLE OF CONTENTS

TABLE OF FIGURES

I. PHASE I SUMMARY

I.A. INTRODUCTION

NASA's Vision for Space Exploration (VSE) relies on numerous systems of systems to support a return of robotic and human explorers to the Moon in preparation for human exploration of Mars. Establishing a sustainable and continuous manned presence on the Moon, Mars, and deep space will require a very large total mass of material to be either launched from Earth, or obtained from the moon or asteroids and made available for structural, propulsion, shielding or other consumable needs. Moving this material in near-Earth and cislunar space using traditional rocket-based propulsion systems requires propellant masses that represent a large fraction of the total required launch mass, and thus cost, of the exploration architecture. The development of reusable, propellantless propulsion technologies could greatly reduce the overall costs of the exploration of space and thus could enable the VSE to evolve into an economically sustainable long-term development of the Moon and near-Earth space.

This Phase I effort has investigated the feasibility of an innovative multifunctional propulsion-and-structure system concept, called Integrated Structural Electrodynamic Propulsion (ISEP), which uses current-carrying booms deployed from a spacecraft to generate thrust with little or no propellant expenditure. This system utilizes methods conceptually similar to electrodynamic tethers with the added benefit of providing a capability for generating thrust in almost any direction as well as for providing torques for spacecraft attitude control. Whereas electrodynamic tether systems typically require very long (multi-kilometer) tether structures, which incur significant dynamics and collision-avoidance challenges, the ISEP concept utilizes several relatively short rigid booms with integrated conductors capable of carrying large currents, as well as components to enable electrical plasma contacts at the ends of each boom. Nominally six of these booms will be connected to a host spacecraft along orthogonal axes, enabling the system to exert control in five degrees of freedom of its motion in space. This integrated propulsion and attitude control structure will facilitate self-assembly of large space systems, and enable propulsion of an assembled system during and after such assembly. By making the system modular, whereby the control nodes and booms are modular and interconnecting, these elements form an innovative Tinkertoy®-like family of components from which larger scale systems can be assembled and reassembled. These modular elements can provide structural support, propulsion, attitude control, and power generation to enable cost-effective on-orbit assembly and operation of large systems such as space power satellites, very-large aperture telescopes and interferometers, resource depots, structures to support ISRU-derived shielding materials, and large space tugs for transporting propellant and resources in support of VSE missions.

I.B. MOTIVATION

NASA's Vision for Space Exploration as given to us by the President's Direction to NASA mandates us to "*implement a sustainable and affordable human and robotic program to explore the solar system and beyond.*" Although NASA's near-term efforts are focused on utilizing mature chemical rocket-based technologies to enable rapid replacement of the Shuttle with the CEV systems, achieving the *sustainable* and *affordable* goals of the VSE for persistent human presence in space will require innovative technologies and reusable infrastructure to dramatically reduce mission costs. A particular problem which continues to plague the space industry is the availability of low-cost propulsion both to provide access to space and for in-space propulsion.

To support sustainable human and robotic exploration, many systems and consumables to support their operation must be delivered to space. Numerous attempts are underway by private ventures to reduce the costs associated with ground based launch systems, and others are researching methods by which in-situ resource utilization (ISRU) can be used to minimize the propulsive delta-V requirements. Still others (including TUI) are developing in-space propulsion systems that minimize propellant usage to transport infrastructure components, payloads, and consumables in space from low-earth orbit to the Moon and beyond.[1] This NIAC Phase I effort has explored and refined the concept of Integrated Structural Electrodynamic Propulsion (ISEP) – a multifunctional structure that incorporates a propulsive element with a rigid boom element that can be used as a structural member either after a propulsive phase of a mission or during a mission as a stationkeeping element.

I.C. ELECTRODYNAMIC PROPULSION

Electrodynamic propulsion involves the use of currents flowing through extended conductors to create thrust forces through Lorentz interactions with a planetary or interplanetary magnetic field. The principles of electrodynamic propulsion were originally discovered during analyses of anomalous drag behavior in the Echo balloon experiments in the 1960's.[2] The vast majority of investigations on electrodynamic propulsion have involved the use of long conducting space tethers, and the basic principles of electrodynamic tethers were demonstrated in the early 1990's in the Plasma Motor Generator (PMG) and TSS-1R[3] flight experiments. More recently, NASA/MSFC developed an electrodynamic tether experiment called ProSEDS,[4] the primary goal of which was to demonstrate electrodynamic tether propulsion. ProSEDS, unfortunately, was cancelled weeks before launch due to ISS-program concerns regarding large orbiting structures. In an orbit-raising electrodynamic tether system, electrical energy generated by solar panels is used to overcome the potential induced on a conductive tether by its motion relative to the Earth's magnetic field and cause current to flow through the tether. The interaction of the current flowing along the tether conductor and the ambient magnetic field produces a force on the tether system that changes its orbit. Since current must flow in a loop, electrodynamic tether systems must include components to collect electrons from the ambient space plasma and emit them back into the plasma, which typically achieved with the use of little or no consumables.[5]

Electrodynamic Tether Limitations: While electrodynamic (ED) tether systems have potential benefits for several applications, the nature of typical ED tether systems also limits their utility for many other applications. Typical electrodynamic tether propulsion system designs require tethers with lengths of 1 to 10s of kilometers, in which currents of 0.1 to 10 amperes are driven to produce thrust levels on the order of several Newtons.[6,7] Electrodynamic tethers also require substantial ambient plasma densities, limiting their operational range to LEO altitudes. Because these long tethers have little or no flexural rigidity, the dynamics of electrodynamic tether systems can be quite complex, and these dynamics result in dynamic effects on the host spacecraft that may not be acceptable for some applications. Furthermore, their long lengths make them unsuitable for use at altitudes used by other high-value assets such as the ISS. Finally, because a tether is long and flexible, gravity gradient forces on the structure will orient the tether along the local vertical direction, and because the direction of electrodynamic thrust is always perpendicular to both the tether and the local magnetic field, an ED tether system is limited to providing thrust along only one axis at any given time.

I.D. INTEGRATED STRUCTURAL ELECTRODYNAMIC PROPULSION (ISEP) CONCEPT

The purpose of the Phase I effort was to investigate an innovative method for implementing electrodynamic propulsion in a manner that may overcome many of the limitations of ED tethers. The first adaptation is the use of short, high-current conductors, rather than long, low-current tethers, to generate thrust. This approach was motivated in part by an analysis by Sorensen that showed that the efficiency of an electrodynamic thruster, given a fixed amount of power available and fixed conductor mass, is independent of the length of the conductor.[8] Consequently, electrodynamic systems using short conductors carrying large currents can produce efficient thrust, *provided these large currents can be exchanged with the ambient environment in an efficient manner*. The second innovative approach is to integrate the electrodynamic component of the system with structural elements which are then coupled to the power generation systems. The basic unit of this system is a lightweight deployable boom that incorporates current-carrying elements along its length, current emission devices at both ends of the boom, and, optionally, thin-film solar arrays mounted along the boom. This multifunctional structure will provide not only virtually propellantless propulsion for a space system, but also act as a structural element for the construction of large space systems and generate power for that system. This forms the basis of a very powerful architecture whereby a system of such system can be constructed.

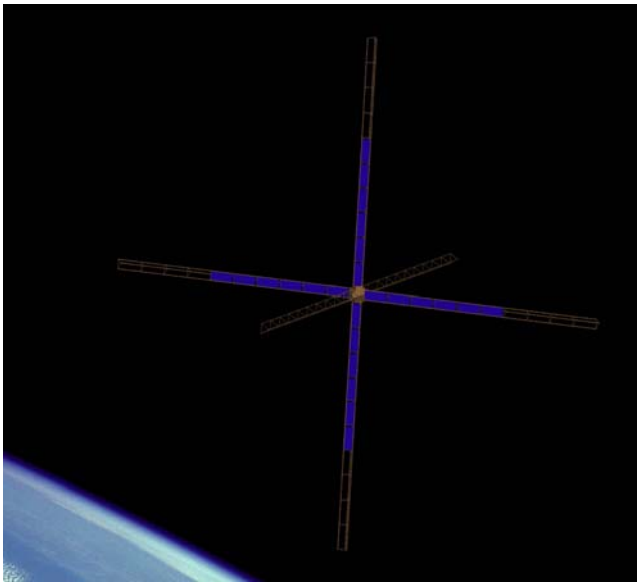

Figure 1. Conceptual illustration of a single Modular Spacecraft with Integrated Structural Electrodynamic Propulsive Elements.

A notional concept for such a system, depicted in Figure 1, consists of a spacecraft in the central location with six 50-meter booms attached to the structure aligned along three orthogonal axes. This forms a baseline of three 100-meter booms with plasma contactors at the tips and near the central spacecraft body. Each of the booms and the plasma contactor elements can be disconnected and reconnected (when current is not flowing) on orbit making the system modular and reconfigurable.

I.D.1 Capabilities and Advantages

The ISEP concept has several unique capabilities and advantages:

- **Orbital Modifications:** A conductor of length and orientation $\vec{L}$ through which a current i flows, when placed into a magnetic field $\vec{B}$, will experience a force $i\vec{L} \times \vec{B}$ due the Lorentz interaction, as illustrated in Figure 2. By modulating the current that flows from boom tip to tip in all three axes, thrust may be generated in almost any direction irrespective of the spacecraft's attitude and the direction of the Earth's magnetic field, other than along the direction of the magnetic field. Even though the electrodynamic technique cannot generate thrust in the magnetic field direction, because the magnetic field magnitude and direction changes as the spacecraft moves in its orbit, the system can still change all six of the spacecraft's

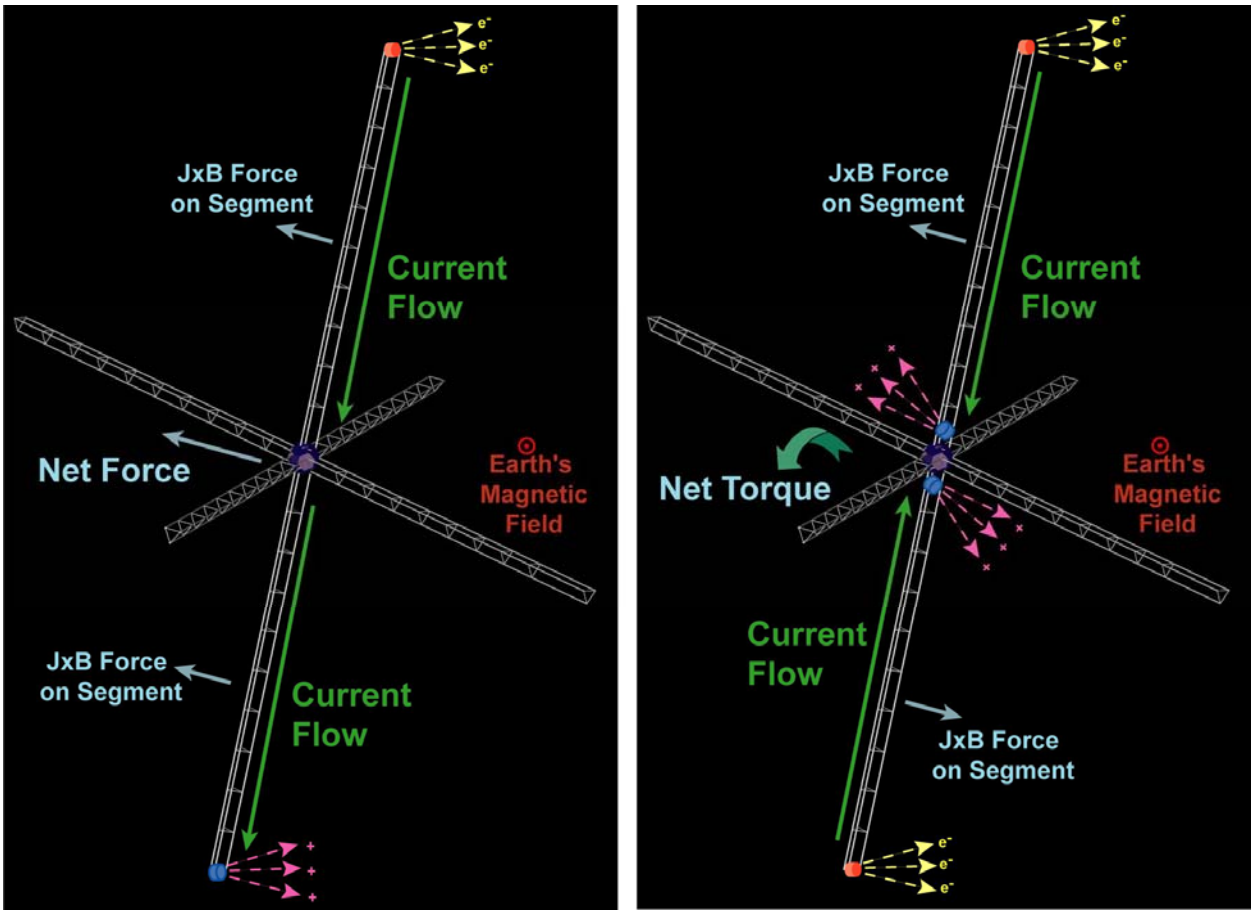

Figure 2. Method by which thrust and torque are generated with the Integrated Stuctural Electrodynamic Propulsion system.

orbital elements by properly modulating the currents over a period of one or more orbits.

- **Attitude Control:** By modulating the current in two halves of an axis independently, the average force on either end will be equal and opposite generating a net torque on the central body and thereby providing the spacecraft with a means for attitude control, as illustrated in Figure 2. Since electrodynamic thrust forces cannot be generated along the magnetic field vector, the torque is also limited to be generated only in the plane perpendicular to the magnetic field vector.

- **Reduced Structural Dynamics Complexity:** Whereas an electrodynamic tether system must incorporate a complex system of sensors and control to maintain dynamic stability of the long, flexible conducting tether, the ISEP concept uses relatively rigid booms to carry the currents and transmit the forces throughout the system. The rigid symmetric structure will reduce the need for the development of complex flexible structure dynamics control as long as the structure is sufficiently rigid to exhibit minimal flex during thrusting.

I.D.2 ISEP Technology Challenges

This unique and innovative approach to Lorentz-force propulsion does not come without its technical challenges. The technical challenges to integrating the ISEP concept into operational space systems include:

A. Efficient collection and transmission of current between the ISEP system and the ambient space plasma;
B. Efficient collection, storage, and processing of energy;
C. Mass-efficient and reliable deployable structures;
D. Formation flying and docking technologies;

Of these challenges, (B), (C), and (D) are not unique to the ISEP concept and these challenges have received substantial attention and investment under other NASA and DoD programs. Challenge (A), that of efficiently contacting large currents to the space plasma is relatively unique to systems that utilize electrodynamic propulsion, including ISEP, the MXER Tether transportation concept, and electrodynamic tethers. Consequently, in this Phase I project we have evaluated technologies relevant to all three challenges and focused our attention primarily upon technologies for making electrical contact with the ionosphere.

High-Current Emission & Collection: Generation of electrodynamic thrust requires transmission of a current in one direction along a conductive element, such as along a boom as illustrated in Figure 3. A critical element of electrodynamic propulsion is the closure of the current loop as required by Kirchoff's Law. In electrodynamic tether systems, this current loop closure is accomplished using passive electron collection by conductors with typically large surface areas, followed by emission of electrons at the other end of tether, and these contacts with the plasma often present the greatest technical challenge in such a system. To produce significant thrusts, an ISEP system must be capable of carrying much larger currents than are typically considered for electrodynamic tether systems. To match the thrust level that a 10-kilometer tether with 1 ampere of current flow in low-earth orbit (LEO) could generate, approximately $|iLxB| \approx 0.3$ N, a 100-meter ISEP boom must conduct 100 amperes of current. To carry this current, the system must be capable of collecting 100 amperes of electron current (or emitting 100 A of ion current) from the ionospheric plasma at one end of the structure and emitting 100 A of electron current (or collecting 100 A of ion current) at the other end of the structure. The technology to efficiently contact such large currents to the ionosphere has not been demonstrated in space. There are, however, several technical options that are likely to lead to feasible solutions, including Field Emission Array Cathodes (FEACs), hollow cathode plasma contactors, and several different concepts for passive current collectors.

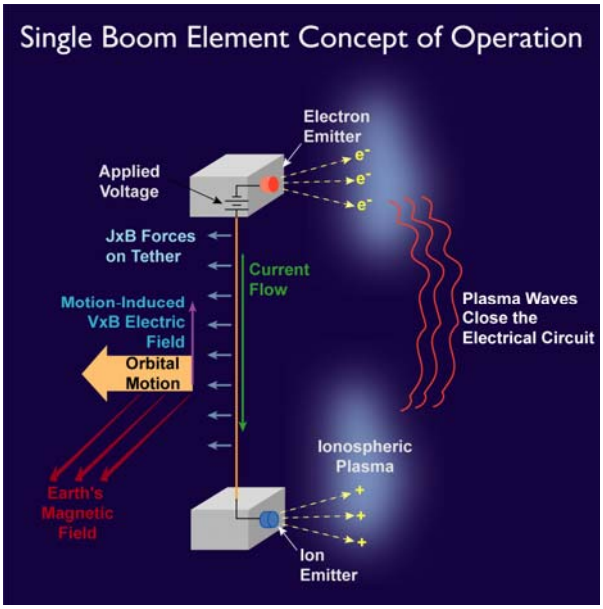

Figure 3. Concept of operations of a single boom element of the Integrated Structural Electrodynamic Propulsion system.

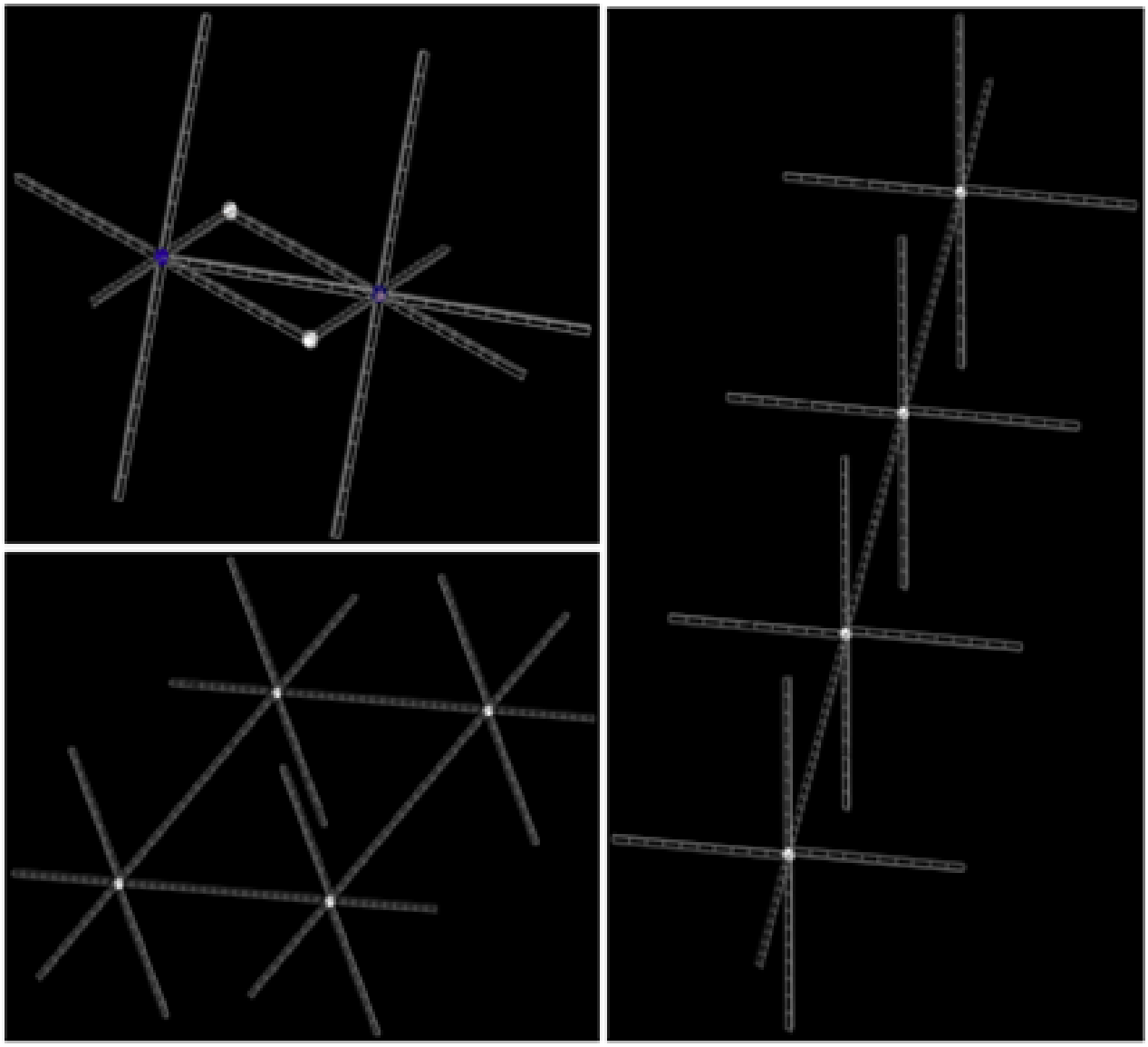

Figure 4. Example assemblies made from modular and interconnectable Tinkertoy®-like power and control nodes and ISEP booms.

I.D.3 Enabled Applications

The proposed ISEP architecture enables a modular approach to constructing large structures in orbit, with the structures themselves providing capabilities for propulsion, attitude control, and power generation. Although a single ISEP element can provide useful propulsion, as illustrated in Figure 2 and Figure 3, this design approach really pays off when two or more elements are combined to create a larger structure, as illustrated in Figure 4. Because the major source of inefficiency in the electrodynamic propulsion system is in the current collection and emission at the ends of the structure, when multiple ISEP structures are linked in series, the net efficiency of the system increases as more modules are added.

The ISEP technology will thus be useful in the construction and operation of space systems that require large structures. Among the candidate applications are:

- **Space Solar Power Satellites (SSPS):** Orbital systems for collecting solar energy and transmitting this energy to ground stations have been proposed as a potential "green" means for satisfying growing global demands for power. Such systems will require the deployment of large fields of photovoltaic arrays or collectors for solar-thermal power generation systems as well as the deployment of very large antenna structures for beaming the power to ground stations. The ISEP architecture could provide a means for deploying these large structures in a modular manner and enabling the modules to self-assemble on orbit.

  An additional potential SSPS approach that the ISEP architecture could enable is solar power satellites that are in non-GEO orbits. Typically, SSPS architectures consider only systems in geostationary orbits, in part to provide continual coverage of a geographic location, but also because the propellant requirements for maintaining the orbit of such large structures in lower orbits would be prohibitive using conventional propulsion technologies. By integrating propulsion capability into the structure, the ISEP technology could enable solar power satellites to be flown in lower, non-equatorial orbits, such as 'MAGIC' orbits[9]. MAGIC orbits are a class of critically inclined, sun-synchronous orbits with 2- or 3- hour periods, so that they have a ground track that is identical every day, that are designed to provide high dwell time over a given geographic area of interest. A system of 6 solar power satellites in a MAGIC orbit could provide continuous power service to a particular ground station. The propellantless propulsion capabilities of the ISEP technology could perform the orbital maintenance of these systems without large propellant requirements, and by enabling the solar power satellites to fly at much lower altitudes, the ISEP technology could greatly reduce the size of the power-beaming antennas necessary to deliver the power to the ground.

- **Large Aperture Radio Telescopes & Interferometers:** Achieving high-priority science goals such as detecting and eventually imaging Earth-like planets around other stars will require telescope and interferometric systems with extremely large apertures and baselines. The ISEP technology will enable such systems to be deployed and built-up in an incremental manner, and can provide propellantless propulsion for assembly and orbit maintenance, as well as attitude control for retargeting.

- **Orbital Tug:** The propellantless electrodynamic propulsion capabilities of the ISEP technology can enable the construction of a system for orbit raising or repositioning of space assets. Such an orbital tug could be used for ferrying propellant tanks, equipment, and other payloads from low-LEO drop-off orbits up to propellant depots or space stations at higher altitudes in support of VSE activities.

- **Orbit Maintenance of Large LEO Systems:** Large LEO systems such as the International Space Station experience constant orbital decay due to aerodynamic drag, and the costs of launching propellant up to these assets to provide reboost capabilities represents a significant portion of their operating budgets. Such systems could instead be constructed using the ISEP technology as their structural backbone, and then the structure of the station itself could be used to provide the drag-makeup propulsion necessary to maintain their orbits. Prior analyses of electrodynamic reboost of the ISS using an electrodynamic tether indicated that cost savings on the order of a billion dollars were possible.[10] The ISEP design approach could enable similar capabilities with the station structure itself serving as the electrodynamic conductor while avoiding the impacts of a tether on station microgravity characteristics as well as upon spacecraft docking and proximity operations.

II. PHASE I RESULTS

II.A. SUMMARY

In this Phase I NIAC effort, we refined the proposed concept of a multifunctional integrated propulsion and structure system that utilizes electrodynamic forces generated by current-carrying booms to generate thrust with little or no expenditure of propellant. To that end, we surveyed the current state of the art in technology areas relevant to the concept's feasibility, and then evaluated the engineering challenges and limitations associated with designing and integrating the various components of the ISEP system and architecture. The technologies of today along with their forecasted performance and capabilities in the future were used to design a notional system consisting of the following components: high performance rigid boom/truss elements with integrated conductive elements for propulsion, modular, fuel and power efficient plasma contactors capable of electron emission, electron collection ad ion emission, electrical energy storage, and modular satellite control nodes with connections ports for the boom system elements. Having surveyed the technologies and designed a notional system and architecture we evaluated key performance metrics of the system to determine technical and economic feasibility of the architecture enabled by the ISEP concept. Subsequently, a number of mission concepts based on the ISEP system and architecture were identified. To further the development of key technologies in support of the ISEP system and future mission concepts, a small experiment was designed that would be performed during the Phase II effort.

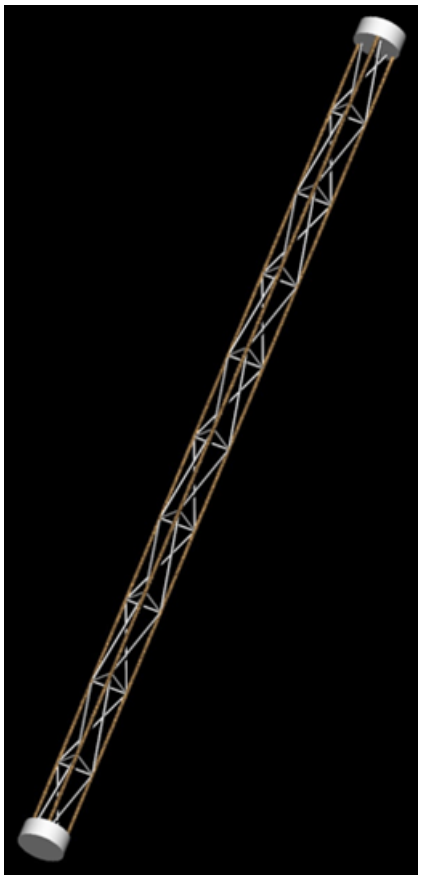

Figure 5. Rendering of a single ISEP element consisting of a structural conductive boom, and two endbodies containing, consumables, avionics, plasma contactors, and hermaphroditic mating interface.

II.B. SYSTEM COMPONENT TECHNOLOGIES

II.B.1 Integrated Structural Electrodynamic Boom

The key element of the Integrated Structural Electrodynamic Propulsion (ISEP) system is this unique combination of a conductor capable of carrying high power with a boom or truss-like structure. TUI has performed considerable work in the area of conductive tethers for electrodynamic propulsion, however the combination of a propulsive element with a rigid structural element is unique to this effort.

In terms of the conductive element through which current will flow, because of the high currents involved, it is very important to minimize the losses in this element as resistive power dissipation is proportional to the square of the current ($P=I^2 R$). In addition to the problem of reduced overall system efficiency, the resistive power losses generate heat, which must be dissipated to keep the resistance in check (almost all good conductors have positive temperature coefficients) as well as to keep the conductive element or its insulation from melting or breaking down. As long as the power dissipated in the propulsive boom element is kept in check, thermal control can readily be accomplished through the use of proper materials and coatings, to have the outer surface of the insulated conductive elements have the desirable radiation and

thermo-optical properties. There is a plethora of materials, coatings and paints[11] that would be suitable for passive thermal control that relies on radiative heat transfer to dissipate heat. To optimize the operations of the ISEP system, it would be desirable to cold bias the conductive elements to minimize the resistance and power loss.

There are a number of material choices available for the actual conductive element of the boom, which are very similar to the materials that TUI considers for conductive space tether applications. For space tethers, the flexibility and handling of the conductive material is quite important as it significantly affects the tether fabrication braiding process, as well as the winding and deployment of multi-strand space tethers. For space tether applications, aramid fibers coated with metals are most often selected at TUI, where the available options today include Aracon® (copper on nickel coated Kevlar) and Amberstrand® (copper on nickel coated Zylon®). These conductive members also offer relatively high breaking strength for higher mechanical load bearing capability.

For the ISEP system, since the current levels are an order (or two) of magnitude higher that is typically considered for electrodynamic tethers, and the flexibility requirement is not as significant, solid and stranded metal electrical conductors can be considered. In exchange for flexibility and strength by using metal wire for conductors, the conductive element can be smaller and more lightweight (see Table 1.) Copper is the most common conductor in use today in virtually all applications, even though aluminum has better conductivity per unit mass and is less expensive. Primarily in the 1960s and 1970s, many electrical contractors used aluminum wiring in residential and commercial buildings as a way to reduce money. Numerous problems with these wiring installations have been discovered, with many of them causing electrical fires. Some of the issues with using aluminum wiring for electrical applications include: aluminum is more brittle than copper, and is more likely to break or crimp which can causing arcing, aluminum expands and contracts more than copper, and oxidation causes the wires to expand which may cause problems with the insulation and stresses at the connection points.

Table 1. Properties of Conductive Materials for Booms, including lineal masses for 50 meter, 0.01 ohm booms (having a resistance of 0.0002 ohms/meter.)

Material	Weight (kg/km)	Material Resistance (ohms/km)	Number of Strands for Target Resistance	Lineal Density (kg/m)
Aracon® XN0400E-018	0.139	3280	16400	2.28
Aracon® XNO200E-025	0.070	9180	45900	3.21
Amberstrand®	1.043	258	1292	1.35
Copper Wire (14 AWG)	18.557	8.3	42	0.78
Aluminum Wire (14 AWG)	5.625	13.5	68	0.38
Copper Clad Aluminum Wire (14 AWG)	6.905	12.7	64	0.44

For the ISEP system to have a nominal power dissipation of 100 watts per 100-meter boom segment with a 100 ampere current, the nominal boom resistance needs to 0.01 ohms. If the conductive material was copper then the conductor would have a mass of 0.78kg/meter, however if the conductive material was aluminum, the lineal mass density would be 0.38 kg/meter. Recently, copper clad aluminum (CCA) wire[12] has entered production that allows one to retain many of the advantageous properties of aluminum wire, with a slight increase in mass. CCA wires are lighter than equivalent copper wires, have a greater flex fatigue life, are lighter than copper, yet still remain compatible with all copper assembly fixtures and processes. A ISEP

boom conductive element of equivalent resistance would have a lineal density of 0.44 kg/meter and a mass of 22kg per 50 meter boom segment.

To minimize the undesired collection of electrons and ions from the ambient plasma, the conductive elements would also be electrically insulated (in addition to having a high emissivity and low absorbtivity surface.) This insulation must be quite good and not trap any residual gasses inside of the insulation, because as it was demonstrated during the anomalous tether break during the Tethered Satellite System 1 Reflight (TSS-1R) mission, the arc that caused the tether to melt and separate was fueled by the residual trapped gas in the 19.7 km long tether. [13] The use of self-passivating materials[14] for the insulation may be required as small breaches in the insulation of a tether exhibit spherical-like current collection characteristics[15], and may pose a challenge the long-term operational health of a ISEP system.

To rigidize the conductive propulsive element of the ISEP system a trussed, beam-like deployable structure will be used. The AFRL, NASA, and DARPA have all invested significantly in research to develop boom and truss technologies which push the limits of structural efficiency to the point where these elements represent a small fraction of total spacecraft mass. Numerous booms and trusses have been successfully flown with demonstrated operation in orbit ranging from booms for instrument isolation (typically magnetometers), to booms for solar cell support (such as the 39m booms on the International Space Station), to supports for antennas for radar applications (the 60m boom flown on the shuttle during the Shuttle Radar Topography Mission, STS-99 in February 2000 is the longest rigid structure ever flown in space).

The design of a boom is driven primarily by three application-dependent operational boom requirements, namely: strength, stiffness, and dimensional stability. Secondary requirements may include reliability, cost, stowed volume and overall mass, as well as a minimum first vibration mode frequency to enhance spacecraft stability and to minimize settling times from maneuvers and perturbations. These requirements will vary greatly depending on the end application be it deployment and rigidization of a solar sail, deployment and support of a phased array antenna or an optical surface, a structural element of a space station. Therefore, an overview of the boom architectures and technologies will be discussed here.

The most influential choices to be made in the design of space booms and trusses are the selection of appropriate architectures, including both the architecture of the boom structure itself,

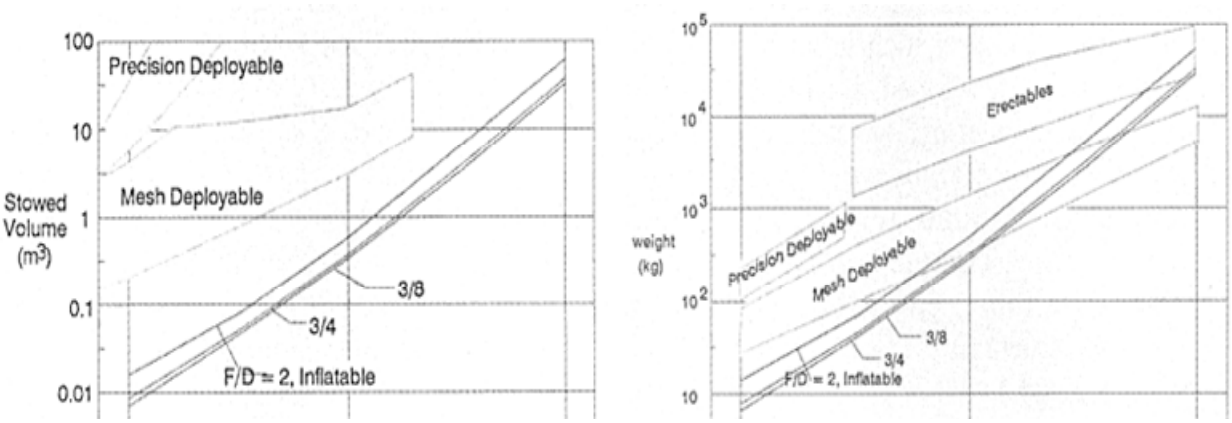

Figure 6. Comparison of stowed volume and mass requirements for deployable space structures. Using various architectures[1]

and the deployment method. Examples of structural architectures include trussed booms, tubular booms, tape-spring structures, and trusses build from solid rod elements. These structural elements can be deployed as inflatable, elastic, rigidizable, or mechanical and hybrid combinations of these[16]. When selecting architectures, the primary tradeoff lies in between simple architectures being less mass efficient with lower risk, with more complex structures being more mass efficient with higher risks. Interestingly, preliminary structural design is often accomplished neglecting the mass of the structure which has proven to be reasonable as the mass of an efficient structure is usually less than the mass of the payload that it supports.[17,18] In Figure 6, there is a comparison of mass and stowed volume of antenna structures constructed using various architectures.

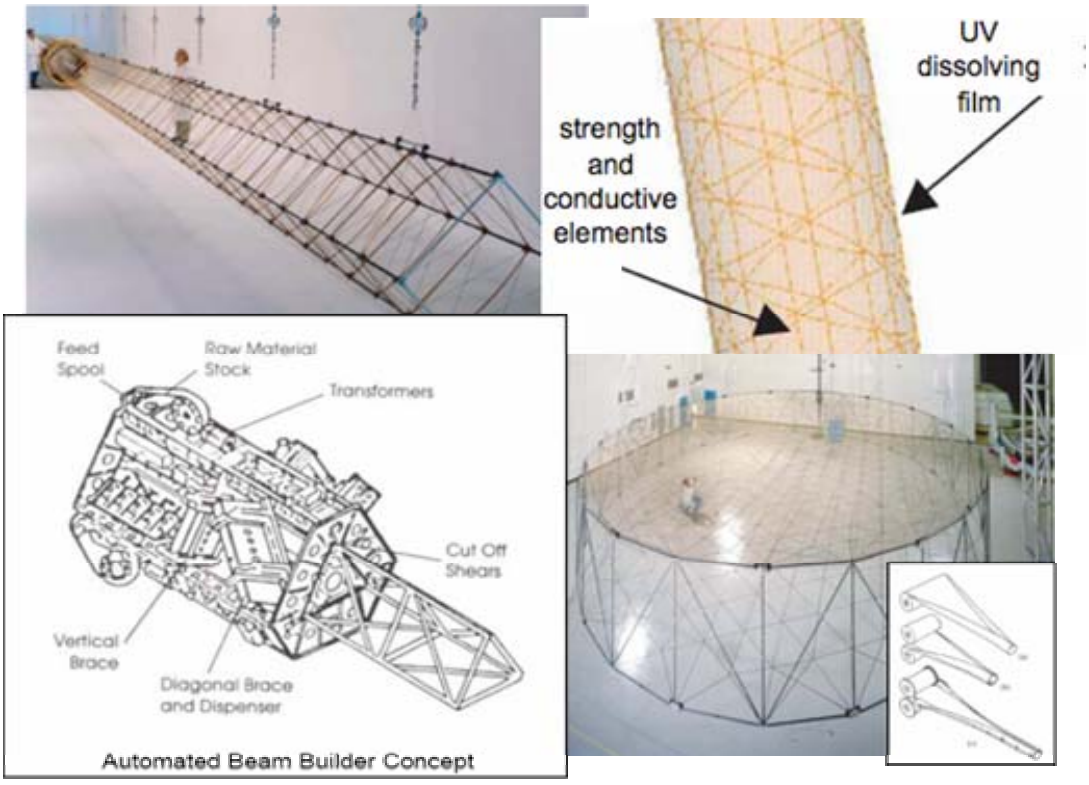

Figure 7. Examples of boom and mesh structure technologies including FAST MAT for the ISS, reinforced inflatable boom, AstroMesh®, STEM, bi-STEM, and interlocking bi-STEM, and an automated on-orbit truss fabrication system.

While there are a number of technologies and solutions available today, it cannot be said that advancements are needed to improve reliability, mass and volumetric efficiencies and reliability. The leading technology candidates of today that could evolve into suitable ISEP structures include the following (some of which that are shown in Figure 7):

- The technology of tensegrity structures (*tens*ile int*egrity*) was patented in 1962 by R.B. Fuller and is commonly described as "an assemblage of tension and compression components arranged in a discontinuous compressions sytem", and is the basis behind very successful deployable technologies in use today such as AEC-Able's FAST mast, and Northrup Grumman AstroMast® and AstroMesh®. This technology can benefit from advances in high-strength materials, composite materials, and innovative structural designs.

- Thin walled tubular deployable/retractable booms constructed of stainless steel, copper beryllium and carbon fibre reinforced plastics are another example of a boom structure that could be used in the ISEP sytem. The Storable Tubular Extendible Member (STEM) was invented in Canada in the 1960s and is an extension of the principle used for coilable and self-straightening steel tape measure booms. This type of structure is well suited for applications mass and volume constraints are critical, with more relaxed stiffness requirements. This type of structure is being planned for use in the Phase II experiment.
- Inflatable structures that typically give the smallest launch package size and potentially the lowest mass are usually constructed from a thin flexible material (often reinforced) which is folded prior to launch and then deployed by inflation. When comparing this technology to other deployable architectures, it important not to overlook the mass, volume and complexity associated with the gas storage and inflation systems. To minimize the adverse effects of micrometeoroid impacts, for most applications the inflatable structures will use some sort of rigidization scheme: foam rigidization, mechanical rigidization, the use of UV cured or thermally cured thermoset resins or composites, or structures that gain stiffness through the work hardening of aluminum laminates. The combination of a UV dissolving film which forms the inflation envelop with thermoset resin coated conductive aramid fibers such as Aracon or Amberstrand for strength and conductivity is quite attractive for the ISEP system.

There exist today suitable technologies and materials to construct and deploy Integrated Structural Electrodynamic Propulsion booms/trusses, however advances in these areas will further reduce the parasitic mass and volume requirements for booms of this system, allowing for an increased payload mass fraction as well as overall increased propulsion efficiency.

II.B.2 Plasma Contactors

In order for the modulated spacecraft with integrated structural electrodynamic propulsion to carry currents along the structures, there must be a way to collect and emit 100+ amps of current into and out of the system. This investigation assesses the current state of the art technology as well as future possibilities to accomplish this feat. A major issue that must be addressed concerns operation of the modular spacecraft outside the ionosphere. In such a location there would not be a source of electrons to collect and an unconventional approach must be used.

II.B.2.i Electron Emission

A survey of electron emission technologies that are critical to Integrated Structureless Electrodynamic Propulsion concept were surveyed, both for the current state of the art, as well as the future development paths.

II.B.2.i.1 Hollow Cathodes

Hollow cathodes (HCs) are the most commonly used device industry as they have been verified experimentally and theoretically for various types of use. The major drawback for this device is the fact that it needs to expend propellant in order to accomplish the desired effect. The basic schematic can be seen

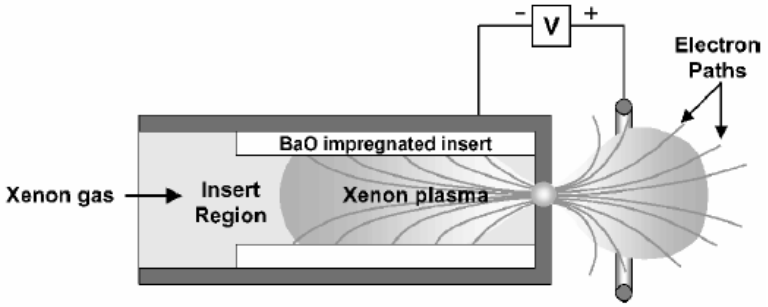

Figure 8: Schematic of a Hollow Cathode.

in Figure 8. Plasma is generated inside the keeper region, usually through thermionic emission. In addition, neutral gas, typically xenon, is sent into the insert region where it is also ionized and then pushed out the orifice. The keeper is biased above the plasma emission at the orifice, which causes the electrons of the ionized plasma to be accelerated. Then depending on the potential of the ambient plasma with respect to the keeper, electron emission, electron collection, or ion emission will occur. Figure 9 shows a description of the current emission or collection depending on the ambient plasma potential. A thorough description of the physics involved for high current HCs can be found in the Hollow Cathode Investigation section of this document.

Numerous companies have been contacted to determine the current state of the art specifications of working hollow cathodes. Table 2 presents a comparison of various hollow cathode devices in the electron emission mode. It can be seen in this table that the power and propellant required to obtain the same amount of emission current can vary greatly. This is due to the fact that geometry and design can play a major role in device power efficiency.

Table 2. Currently Available HCs for Electron Emission.

Company	Consumable Mass Flow Rate	Emission Current	Discharge Voltage	Power	Primary Fuel Type
Busek	40 sccm (3.9 mg/sec)	100 A	25 V	2500 W	Xenon
Aerojet[19]	50 sccm	60 A	11 V	660 W	Xenon
HeatWave Labs	10 sccm	100 A	100 V	10000 W	Xenon
HeatWave Labs	5 sccm	100 A	100 V	10000 W	Argon
JPL[20]	9.5 sccm	100 A	27 V	2700 W	Xenon
NASA Glenn[21]	20.5 sccm (2 mg/sec)	100 A	12.5 V	1250 W	Xenon
JPL[22]	9 sccm	100 A	24 V	2400 W	Xenon

The mass flow rate is also a limiting factor to this technology. Using the NASA Glenn HCs, it would take approximately 20.5 sccm (standard cubic centimeters per minute) of fuel to emit 100 A worth of electrons. As typically the xenon atoms are singly ionized, it would take ~2 mg/s worth of propellant to operate (1 sccm of Xe equals 0.098 mg/sec.) An alternative method to emitting Xe atoms is the emission of hydrogen atoms. The purpose of HCs for this application is to emit current, not mass, so the use of hydrogen would produce the equivalent emitted current. As t 1 sccm of hydrogen corresponds to 7.4 x 10^{-4} mg/s, it can be determined that only 0.015 mg/s are needed. This reduces the fuel requirement by a factor of 132 at the expense of increased handling complexity due to the explosive nature of hydrogen case (especially in ground testing environments). The annual fuel requirement for a

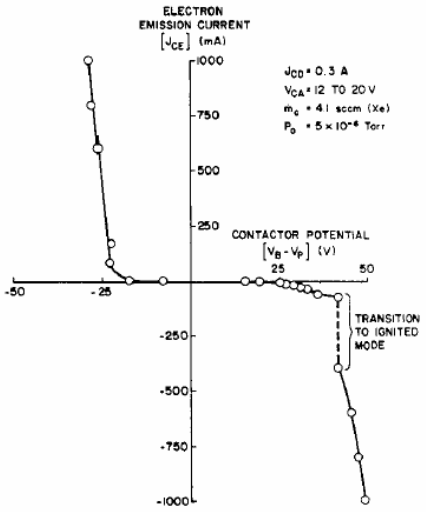

Figure 9: Typical current vs. voltage (I-V) plot of a hollow cathode emitter.

hollow cathode emitter is either 61.6 kg of xenon, while the same system only requires 0.47 kg for hydrogen. Further hollow cathode analysis can be found in an appendix of this document.

II.B.2.i.2 Field Emissive Arrays (FEAs)

In field emission array cathodes (FEACs), electrons tunnel through a potential barrier, rather than escaping over it as in thermionic emission or photoemission. For a metal at low temperature, the process can be understood in terms of Figure 10. The metal can be considered a potential box, filled with electrons to the Fermi level, which lies below the vacuum level by several electron volts. The vacuum level represents the potential energy of an electron at rest outside the metal, in the absence of an external field. In the presence of a strong field electrons are extracted from the conduction band.

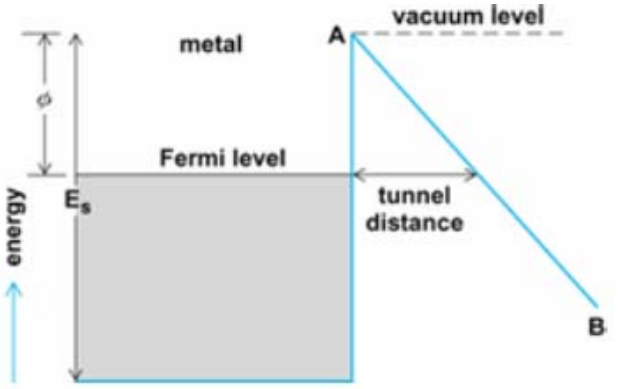

Figure 10: Energy level scheme for field emission from a metal at absolute zero temperature.

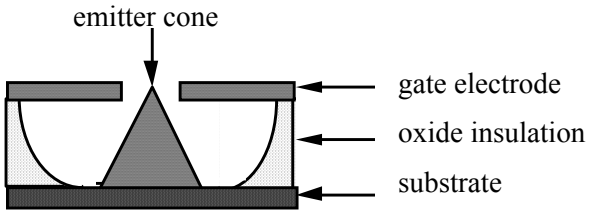

Figure 11: Single Field Emitter Tip Schematic.

The emitted current from a field emitter array can be modeled by the Fowler-Nordheim equation, given in Eq. 1, which dictates how much current can be emitted by an FEA given the potential across the gate to tip gap.[23] A schematic of the FEA can be seen in Figure 11. For this model, the parameters A and B are constants that must be experimentally determined by the emitter material in units of A/V^2 and V respectively, to get an value J for the emitted current density. It turns out that each individual FEA device has its own specific constants based on its particular design which must be derived from the performance curve. The photos in Figure 12 are scanning electron microscope (SEM) images of SRI International's FEAs pioneered by Capp Spindt[24] actual pictures of the technology, detailing the sizes involved in such manufacturing.

$$J = A \cdot V_{emit}{}^2 \cdot e^{-B/Vemit} \qquad \textbf{Eq. 1}$$

The FEA technology presents the greatest potential for propellantless propulsive capabilities of this modulated spacecraft concept. The power requirements for this device are very low, theoretically requiring only ~60 V to emit up to 10 A or electron current. The major drawback is that this technology is sensitive and has not been tested in space rigorously. FEA's have been experimentally tested in a laboratory setting and shown to work at 1 cm^2 of surface area with 1,000,000 tips. In contrast with single device emitters, FEA cathodes offer a great deal of redundancy as there are typically 10s to 100s of thousands of array in a single device, meaning that if some are damaged, there would be numerous others that will continue emitting. Caution is their operation and use is required, as should a few volts potential above the maximum be applied, and all the tips could be damaged.

According to Kevin Jensen's FEA theory, a FEA device has been proposed that can emit up to 10 A of electron current. The specifications of it can be seen in Table 3. It can be seen that the parameters of this device are much greater than anything that has been significantly different from the devices to date, however are within reason for a mission many years in the future.

Table 3. Kevin Jensen's Theoretical 10 A FEA Specifications.

Tip Density	20,000,000 tips / cm^2
Total Area	650 cm^2 (14.38 cm rad circle)
Fowler Nordheim Constant A	37286 A/V^2
Fowler Nordheim Constant B	962.5 V
Min / Max operating potentials	33.1 V / 58.8 V
Area of Emitter	650 cm^2

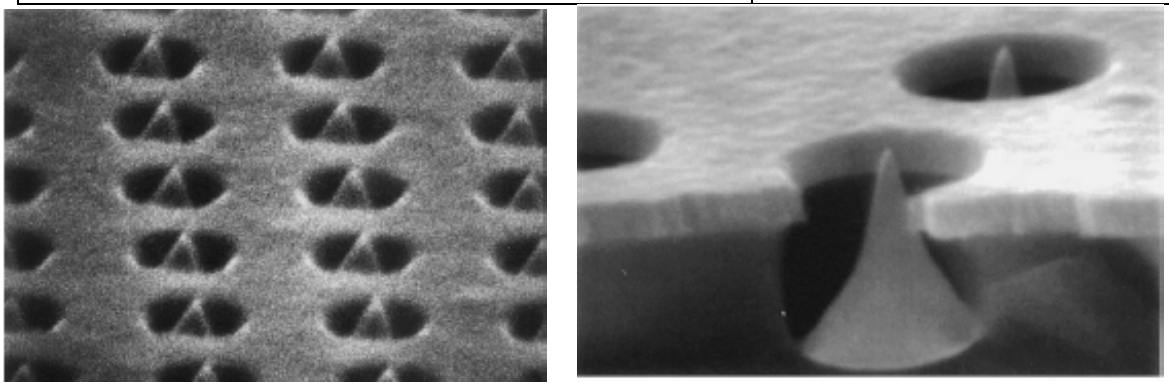

Figure 12. Scanning Electron Microscope (SEM) images of FEA and single tip section.

Theoretically this would work, however it would require 10 FEAs to emit 100 amperes of electrons. In addition, the devices would need to be kept within 0.4 V of the plasma potential or else the effects of space charge limits (SCL) would cause the electrons to reconnect with the device and spacecraft, greatly limiting the amount of emitted current. The devices would also have to be spaced far enough apart from each other so that the effects of space charge limiting would be minimized. To emit 100 amperes of electron current from an array of these devices would require approximately 5.86kW of power.

II.B.2.i.3 Thermionic Cathodes

The emission of electrons from a thermionic cathode (TC) is calculated in a similar way to the emission from field emissive arrays.. The major difference between the two technologies is that the thermionic cathode is a two part system: the thermionic emitter followed by a focusing electron gun. The performance of the thermionic emitter component (an example is show in Figure 13) is dictated by the Richardson-Dushman equation, as seen in Eq. 2.[25] The number of electrons that get released are dependent on the material temperature T (eV), the emitter material work function φ, and a constant *A* determined by the emission material). Following the emission, the electrons are then accelerated by an electron gun (see Figure 14) into the plasma. The electron gun emission I_{eg} can be modeled by Eq. 3, which is takes into account the emission efficiency η, the geometry of the device as a perveance ρ, and the acceleration potential V_{eg}.[26]

$$J = A \cdot T^2 e^{-\left(\phi / qT\right)} \qquad \textbf{Eq. 2}$$

$$V_{eg} = \left[\frac{\eta \cdot I_{eg}}{\rho} \right]^{2/3} \qquad \textbf{Eq. 3}$$

From Eq. 2 it can be seen that the thermionic emitter can regulate the amount of electron produced for then the electron gun to accelerate, by controlling the temperature. This means that the emissions of a thermionic cathode can reach a temperature limiting case, whereby the electron gun potential would increase but the emission current would not, if the thermionic emitter did not produce enough electrons.[27]

Figure 13. Photo of a thermionic emitter.

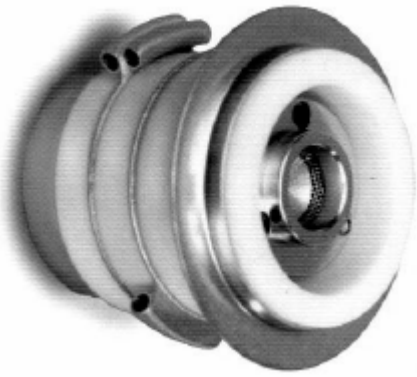

Figure 14. Photo of a TC electron gun.

This technology has been proven to work in the laboratory as well as in space aboard the TSS-1R mission.[27] A major benefit to this technology is that it requires no fuel like the FEAs, however demonstrated current levels have been well below the 100 A target. The state of the art cathode from HeatWave Labs Inc. can generate up to 5.7 amperes of electrons. To generate 100 A of current 18 emitters would be needed, running in parallel and with the accelerating potentials being on the order of 20kV, a total power of 2100 kWatts would be required for this device to operate alone. To minimize the effects of space charge liming the emitters must also all be within 1.25V of the plasma potential. The high power required here, does not suggest that this is a viable option for the ISEP system.

Table 4. HeatWave labs Inc. 5.7A thermionic cathode specifications.

Thermionic Emission Operating Potential	6.3 V
Richard Dushman Constant *A* for Tungsten	120 A/cm^2
Work Function	3.2 eV
Perveance	2 µpervs
Electron Gun Potential	20 kV
Efficiency Factor	0.97
Emitter Area	0.317 cm^2

II.B.2.ii Electron Collection and Ion Emission

To complete the circuit, and minimize any adverse spacecraft charging effects, either electrons must be collected or ions must be emitted at the other end of the ISEP booms. A survey of electron collection and ion emission techniques and technologies that are critical to Integrated Structureless Electrodynamic Propulsion concept were surveyed, both for the current state of the art, as well as the future development paths.

II.B.2.ii.1 Passive Electron Collection

Passive electron current collection I_e, can be readily accomplished by positively biasing a collective surface by a positively biased conductor with respect to the plasma. To model the current that a spherical surface can collect, we will utilize the Parker Murphy Equation.[28] Specifically, a corrected version of this equation based on mission data from the TSS-1R mission (which demonstrated greater than previously predicted current collection which was accommodated by changes in α and β), is used in the spreadsheet and shown in Eq. 4 and Eq. 5. In the Parker-Murphy model, I_o is the electron thermal current density scaled by the area of a hemisphere $2\pi r_s^2$, w is the gyro-frequency, and α and β are constants.[29] For the Parker-Murphy model to be valid in predicting collection, the following conditions must hold:

1) The cyclotron radius is small with respect to the collector,
2) The electron current being collected does not deplete in any way,
3) Spherical conducting body,
4) Conservation of angular momentum,
5) Collisionless plasma without ionizations,

$$\phi_o = \frac{m_e \cdot w^2 rs^2}{8 \cdot q} \qquad \textbf{Eq. 4}$$

$$I_e = \alpha \cdot I_o \cdot \left[1 + \left(\frac{V_{sh}}{\phi_o} \right)^{\beta} \right] \qquad \textbf{Eq. 5}$$

While the Parker-Murphy equation models collection by a solid spherical surface, some work has been done to calculate the currents collected when the solid sphere is replaced with a gridded porous one to minimize atmospheric drag.[30] Current results to date suggest that the currents collected are comparable but lower than that for a same sized sphere. Overall, the passive collection of electrons requires either significant power or significant surface area when tens of amperes of electrons are needed.

For example, a 1 meter radius sphere would require 4.6 MW of power to collect 100 A, with a corresponding drag force in the range of 6.6 mN (or 0.7 mN for a 90% porous sphere). To reduce the amount of power required, the sphere can be enlarged, and with 1 megawatts of power, a 2.29 meter sphere can be used, which would experienced 35 mN of atmospheric drag (or 3.5 mN for a 90% porous sphere).

II.B.2.ii.2 Hollow Cathodes

As mentioned earlier, HC's are theoretically and experimentally used for electron collection and and can theoretically be used for ion emission for currents up to 100 A. Ion production rates are typically on the order of 10 A, as the ratio for electron current collection to ion emission is

approximately 10 to 1. The use of hollow cathodes as purely an ion source is still being investigated as it is a very inefficient process. Hydrogen fuel is being investigated because the mass requirements are significantly less. TO achieve emissions of 100 amperes, approximately 1400 sccm of fuel is required, or about 137 mg/s Xe or 1 mg/s H for 100 A. The specifics of HC electron collection and ion emission are presented in a later section.

II.B.2.ii.3 Ion Source / Ion Gun

This method required a technique similar to the thermionic cathode system in that an ion source is required to extract the ions from the neutral gas, and then an ion gun is used for the emission. There are very few reasons to produce ion currents up to 100 A for any application, and as a result most ion emission systems designed in industry are for low currents. For example, HeatWave Labs Inc. has an ion emission system that can emit 1.2 mA with an applied 10kV potential. In order to achieve 100 A, 83,334 emitters will be needed and a power supply of 1 MW, along with a high gas flow rate. Due to this fact ion emission physics needs to be investigated in order to obtain some theoretical numbers for emission up to 100 A.

$$K_{iz}E_c = K_{iz}E_{iz} + K_{ex}E_{ex} + K_{el}\cdot\frac{3m_e}{M_i}\cdot T_e \qquad \textbf{Eq. 6}$$

According to Lieberman & Lichtenberg the energy loss per electron-ion pair created is summed up in Eq. 6.[31] The complete energy needed for each pair is calculated by the sum of the energies needed for the ionization, the excitation and the elastic scattering. 'K' is the rate constant [m^3/s], E is the energy, and $(3m_e/M_i)T_e$ is the mean energy lost per electron for polarization scattering. Each of the terms is dependant upon the electron temperature, T_e, which can be calculated using reaction equations as seen for argon and oxygen (Lieberman table). Using argon as the fuel, for T_e values over 15 V the total E_c value is constant at about 20 V, and for T_e values between 1 and 15 E_c ranges from 18 to 1000 V. (the ionization energy for argon is 15.759 eV). Typical T_e values inside an ion emitter will be over 40 V, and as a result the energy loss involved in creating an ion is on the order of 20 V.

Similarly for xenon, the ionization energy is 12.13 eV, and since it is a noble gas is expected to perform comparable to argon, possible slightly less because of the 3.5 V less ionization energy. For the purposes of this phase of the project assuming the value remains unchanged, which means to emit 100 A of ion current at 16.5 V a collision, will require approximately 1,650 W of power to maintain the constant ionization, assuming 100% ionization of the feed gas. When ionizing a molecular gas such as hydrogen, there are other issues that must be considered. Additional collisional energy losses are present in these gasses, including excitation of vibrational and rotational energy levels, molecular dissociation, and, for electronegative gases, negative ion formation. As a result, the E_c value can be a factor of 2 to 10 times greater than for a noble gas of the same T_e, when it is below ~20 V. In this case it would not affect the results as the temperatures being dealt with are above that threshold. For comparison purposes, as the ionization energy for hydrogen is 13.9 eV, which results in a total required power of 1830 W for 100 A ion emission.

II.B.2.iii Space Charge Limiting

Any system that emits electrons at sufficiently high densities for particular electron energy level will ultimately face the space charge limit (SCL) or the point at which the electrostatic force from the cloud of emitted electrons becomes sufficient to decelerate and ultimately reflect the electrons being emitted to the ambient plasma. This limit is especially important where the

power that is to be expended to emit electrons to the ambient plasma is at a premium, as is the case for spacecraft utilizing electric propulsion, electrodynamic tether propulsion as well as the ISEP booms for propulsion. In particular, space charge limits need to be considered with utilizing field emissive array cathodes as they are inherently capable of high-current and low-power emission without the benefit of consumables.

The SCL of a FEA is calculated for an ion collection sheath around an end-mass that has a negative potential with respect to the plasma (a positive potential here would mean that the electrons that are trying to be emitted would not only have to overcome the SCL, but the attraction of a charged body pulling them back). The ion sheath radius r_{sh} calculation is conducted using a method developed by Parker, using in Eq. 7, Eq. 8, and Eq. 9.[32] The key parameters to compute the dimensions of the sheath include: V_{sh} - the potential across the sheath in Volts, J_{bohm} - the Bohm corrected ion thermal current[33], and the radius of the conducting sphere r_s, (with fundamental physical constants electron charge q, the ion mass m_i and permittivity constant e_o.) The important limitations for this model include the following assumptions:

1. The conductor (the emission endmass) is a sphere,
2. Particles move radially inward from an outward emitter (the ambient plasma),
3. The particles have no angular momentum,
4. The result is not valid if the sheath size is comparable to or exceeds the dimensions of the body.

$$t_u = \frac{2}{3}\sqrt{\left(\frac{2\cdot q}{m_i}\right)^{1/2}\left(\frac{e_o \cdot V_{sh}^{3/2}}{J_{bohm}}\right)} \qquad \textbf{Eq. 7}$$

$$H_u = 0 \; If \cdot \left(\left(\frac{t_u}{r_s} - 0.2\right) < 0\right), \; else \; H_u = 1 \qquad \textbf{Eq. 8}$$

$$r_{sh} = r_s \cdot \left(0.5 + \sqrt{0.25 + \frac{t_u}{r_s}} + 0.052 \cdot \frac{t_u}{r_s} \cdot H_u\right) - r_s \qquad \textbf{Eq. 9}$$

Once the dimension of the ion sheath r_{sh} has been calculated, the SCL can now be calculated using the 1-D classical Child-Langmuir Law[34] as given by Eq. 10 where V_{emit} is the acceleration potential across the emitter, A_e is the emission surface area. The use of this model to predict the space charge limit assumes that:

The electrons are non-relativistic,

1) The motion is one-dimensional,
2) The self magnetic field is negligible.

$$I_{CL}(1) = \frac{4\varepsilon_o}{9q}\sqrt{\frac{2}{m_e}}\frac{V_{emit}^{3/2}}{r_{sh}^{\;2}}\left[1 + \sqrt{1 + \frac{V_{sh}}{V_{emit}}}\right]^3 A_e \qquad \textbf{Eq. 10}$$

Improvements to the space charge limit can be had when considering the spreading of electrons emitted in multiple dimensions, and most significantly depends upon the width of the emitter as

compared to the emission gap. The most reasonable approximation of space charge limit from a flat circular FEA with a radius r_b emitting an expanding 'pencil-beam' is commonly calculated using Eq. 11.[35] This model assumes that:

1) The emitter is a flat and circular with radius r_b,
2) The gap size is greater than the radius of the emitter,
3) There is beam spreading,
4) The emitter area is in isolated 1 cm^2 sections spaced such that the gaps between emitters is on the order of r_{sh}.

$$\frac{J_{CL}(3)}{J_{CL}(1)} = \frac{\left[r_b^2 + (r_{sh}/2)^2\right]}{r_b^2} = \left[1 + \left(\frac{r_{sh}}{2r_b}\right)^2\right] \qquad \textbf{Eq. 11}$$

Alternately there is another 3-D space charge limiting model which describes emission flow coming from a planar ellipse with semi-major axes of *R* and *W/2* seen in Eq. 12.[36] The constraints on the validity of the model are:

1) Planar elliptical emitter where *R > W/2,*
2) Does not give correct limits when W and R approach zero.

$$\frac{J_{CL}(3)}{J_{CL}(1)} \cong 1 + 0.32\frac{r_{sh}}{W} + 0.091\frac{r_{sh}}{R} \qquad \textbf{Eq. 12}$$

Both of the aforementioned 3-D models can be used to calculate the space charge limits of emissions from field emissive array cathodes as well as hollow cathodes. The geometry of the emitter will dictate which 3-D model needs to be used. When considering multiple emitters, one computes the space charge limit for a single device and relies on the geometric placement of the emitters to ensure that their beams do not interact.

Numerous techniques have been recently investigated in an effort to reduce the effects of the space charge limit on electron emission from FEAs, including variations of the emitter size and spacing, the addition of defocusing rings, and temporal and spatial modulation of the emitted beam[37]. The separation of large emitters into multiple small emitters so that the beams do not interact produced the greatest improvement, without having an excessive negative impact on emission power and mission integration costs. The use of defocusing rings was found to increase emissions from small emitters by as much as 40% even when the rings were a simple grounded ring. The use of temporal modulation was not very effective at increasing emission levels unless the FEA was operated at levels beyond the space charge limit, and even then the system was constrained by the same time-averaged space-charge limit. In addition the use of dual grids with FEAs has been investigated with the result that if the system is designed to minimize grid currents, then the power required to effect electron emission can be reduced significantly[38]. This technique can be used to improve the efficiency of the overall system or alternately in cases where available power is fixed, the additional power can be used to increase the energy of the emitted electrons thereby effectively increasing the system's space charge limit.

II.B.2.iv Plasma Contactor Summary

The comparison of the technologies considered and surveyed is summarized in Table 5. As one of the primary goals of the ISEP system is to minimize the reliance on fuel or propellant, based on the state of the technology to date, and the projected and expected development paths, the use of field emissive arrays for electron collection and the use of a hollow cathode for electron collection seem to be the best solution. There are options to truly make the system propellantless, however the power requirements are quite high and it may be more cost effective to include a (relatively) small amount of propellant into the system.

Table 5. Comparison of electron emission and electron/ion collection at 100 A.

Emission	Device	Power	Notes
Electron Emission	TC + Electron Gun	2.1 MW	18 emitters, < 1.25 V for SCL
	FEA	5860 W	10 emitters, < 0.4 V for SCL
	HC	1250 W to 10 kW	Flow Rates & Ion Type 9 sccm to 40 sccm Xe
Electron Collection	Passive Sphere a	4.7 MW	1 m radius, 6.6E-3 N Drag 90% Porous – 6.6E-4 N
	Passive Sphere b	1 MW	2.29 m radius, 3.46E-2 N Drag 90% Porous – 3.46E-3 N
	Passive Plate a	61.3 MW	5 m^2 – 5.26E-5 N Drag
	Passive Plate b	1 MW	54.52 m^2 – 5.73E-4 N Drag
	HC	6150 W + 330 W (20 A ion prod.)	280 sccm fuel 27.35 mg/s Xe^+ or 0.21 mg/s H^+
Ion Emission	Ion Emission + Ion Gun	1 MW + 1650 W (100 A ion prod.)	83,334 emitters needed
	HC	1000 W + 1650 W (100 A ion prod.)	1400 sccm fuel 27.35 mg/s Xe^+ or 0.21 mg/s H^+ **Investigating SCL for low n_p

For nearer term and short duration applications, the use of hollow cathodes should be considered as the performance and reliability of high current cathodes both for electron emission and electron collection have been demonstrated repeatedly both in ground space simulation chambers and space flight missions. The most significant tradeoff here is that the use of xenon gas is required; however hydrogen also needs to be considered in the trade studies as it is 139 times less massive. It does need to be mentioned that when this system will be used outside of the Earth's ionosphere the hollow cathodes will have to be used in ion emission mode to achieve current closure.

II.B.3 Docking Mechanisms and Sensors

At each end of the structural elements are endbodies that house the plasma contactors along with their fuel, and the system elements that support docking of the ISEP booms with other elements of the system. Figure 15 shows a concept design for a mating interface that would be located at the distal end of the boom. This interface contains the docking mechanism as well as the sensors that can be used to aid in the autonomous navigation in the docking phases. This docking mechanism design is hermaphroditic, maximizing the flexibility of the system, and provides mechanical as well as electrical interfacing both in a boom-to-boom configuration as well as boom-to-node. The electrical interface is complicated by the need for high current, high voltage

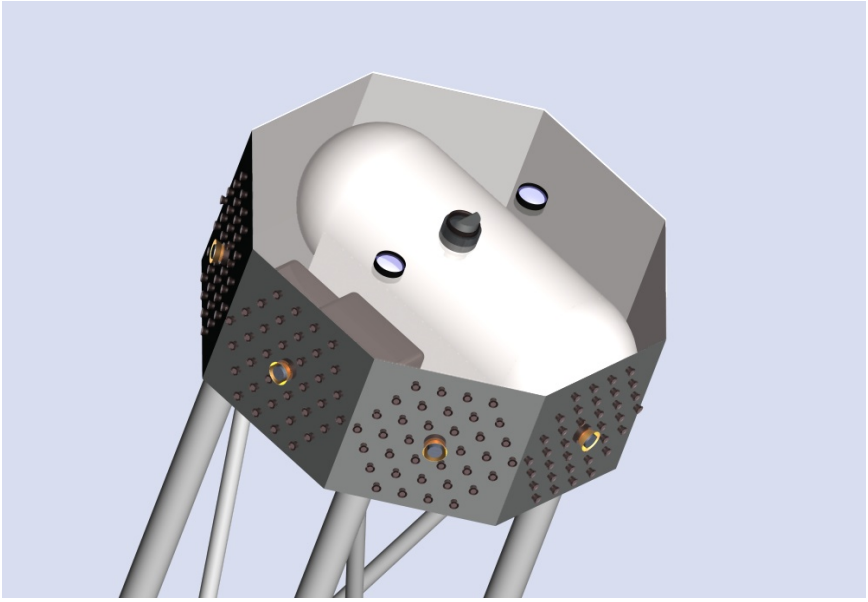

Figure 15. Concept design for the structural element endbody (with transparent lid for visibility).

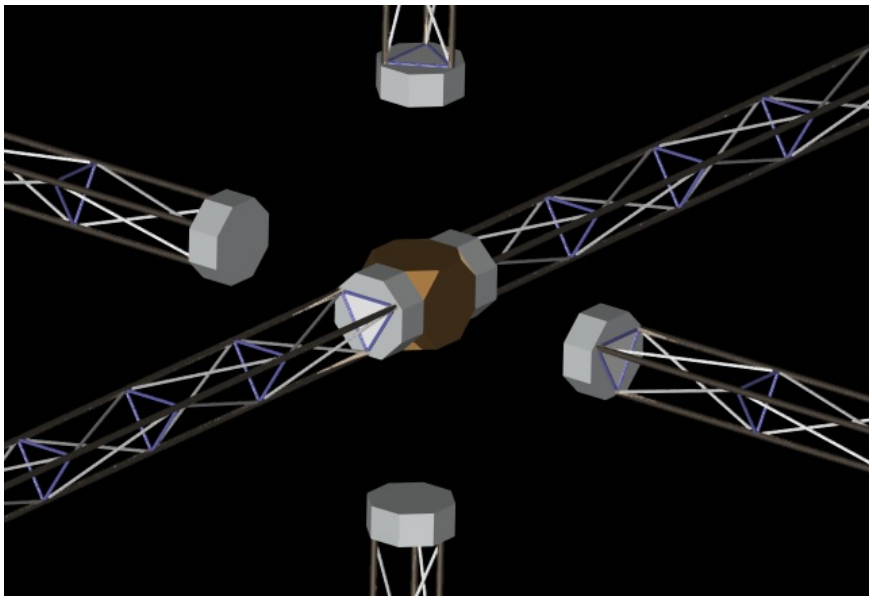

Figure 16. Node with 6 mounting surfaces.

connectivity between nodes as well as communication and control signal lines. Each one of the ISEP boom endbodies also contains the consumable material used to support the discharge in the plasma contactors, and should there be a desire to allow for gas transfer between booms, an addition gas transfer interface would have to be added.

The conceptual design of the ISEP endbodies has an octagonal cross section upon which are mounted the plasma contactors. Each one of the faces has a single hollow cathode emitter along with multiple FEA devices, which have been place with maximal separation to help reduce the limitations associated with space charge limiting. To maximize performance over the lifetime of the system and to increase the system's overall reliability, the current configuration has redundancy built in with more contactors than needed to generate 100 amperes of current.

In their most simple form, a node provides 6 orthogonally aligned mounting surfaces (see Figure 16) with an interface that matches the ISEP boom endbodies (hermaphroditic mechanical and electrical connections, etc.) Each of these nodes contains an electrical energy storage system, and avionics for communication, commanding and control. For an ISEP system to be operational, at least one node will be needed, since the booms themselves have little or no intelligence for autonomous flight. Through the inclusion of gas line interfaces and plumbing, it is possible to have the nodes transfer gasses from one node to another to equalize fuel consumption in an operation ISEP system.

A number of applications of this system have been identified where the ISEP architecture would benefit from configuration options other than simply having orthogonally aligned booms. An example node geometry with additional facets on the surface that would allow docking not only along the Cartesian orthogonal axes but also along 45 degrees along three orthogonal circumferences is depicted in Figure 17

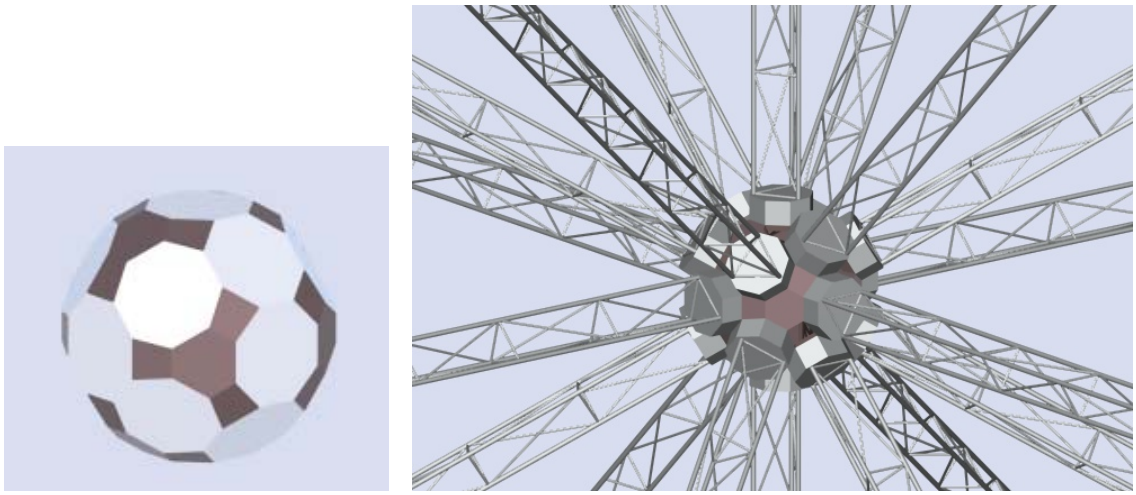

Figure 17. An example node with docking surfaces every 45 degrees, and an example of a fully populated node..

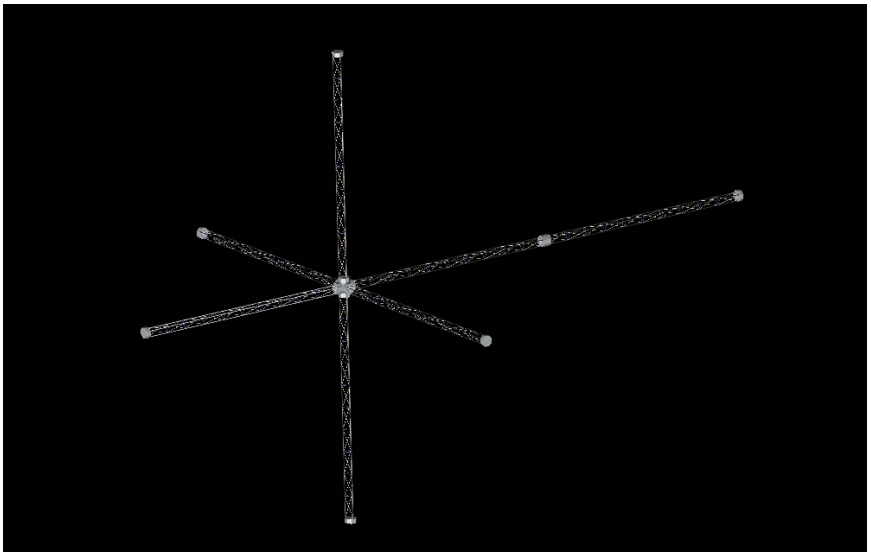

Figure 18. Possible configuration with a 6 position node and a single endbody to endbody attachement.

II.B.4 Electrical Energy Storage Subsystem

As can be seen by the power requirements of the plasma contactors as summarized in Table 5, the operational power demands of the ISEP system are quite high. Short of having nuclear power source onboard, which is quite unlikely in the current political and environmental lobbying environment, power for propulsion will most likely be converted from incident solar power. Since one cannot be guaranteed constant solar illumination in most of the orbits of interest to the NASA Vision for Space Exploration, incident solar energy must be converted to electrical energy for storage and use.

Since the introduction of electricity into society, the cost, capacity and technology of stored electrical energy has played a critical role in the development of electrical and electronic devices. Many of today's devices and appliances in everyday use is highly most notably cellular

Table 6. Comparison of electrical energy storage technologies.[39]

	Nickel Metal Hydride Batteries	Lithium Ion Batteries	Near Term Flywheel Systems	Future Flywheel Systems
Cell Energy Density	35-55 whr/kg	70-150 whr/kg	24-40 whr/kg	50-75 whr/kg
Device Capacity	20-300 A-hr	20-60 A-hr	> 4kW-hr	> 20kW-hr
Operational Depth of Discharge	30%	10-15%	90%	90%
LEO Service Lifetime	5-7 years	5-7 years	15 years	> 15 years
System Energy Density	5-10 whr/kg	10-30 whr/kg	10-20 whr/kg	40-75 whr/kg

telephones, cordless telephones, portable music devices such as the iPod and laptop computers are not only dependent on electrochemical energy storage, but also highly limited in their use due to their low capacity. In addition with the recent increases in the gasoline prices, the demand for electric-powered has greatly increased. With current energy storage devices and systems the electric powered automobiles suffer from limited driving range, short battery service lifetimes, and sluggish acceleration, which is partially resolved in today's hybrid gas/electric vehicles. Nevertheless, these powerful markets are driving the development of improved power storage technologies and power sources such as fuel cells.

A number of years ago, engineers at the NASA GRC Power and Propulsion Office embarked on the development of flywheels for electrical energy storage with the goal of obtaining a leap and future development path in the energy storage densities beyond what was being projected for electrochemical cells. A flywheel is a device that stores mechanical energy in the form of a rapidly (60,000-100,000 rpm) spinning rotor. The device is "charged" by by spinning the rotor to its maximum velocity using an integral motor/generator in the 'motor' mode. It is the "discharged" by using the same motor/generator in 'generator' mode to draw out the kinetically stored energy. Advances in high strength fiberbs and composites have boosted the device capacity by allowing stronger, lighter,

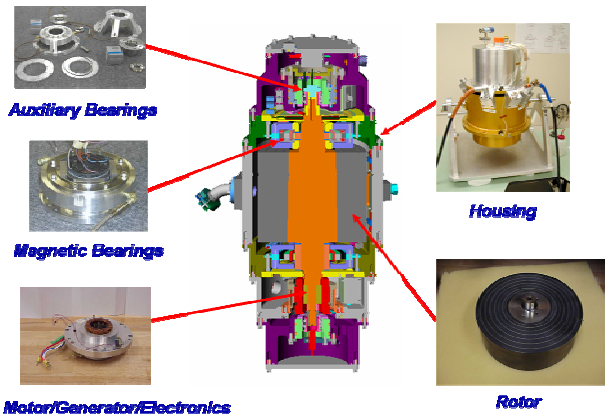

Figure 19: Component technologies of NASA GRCs G2 developmental flywheel.

rotors to be constructed. Advances in magnetic bearings have allowed these rotors to be safely and higher velocities with lower losses, that are dominated not by mechanical friction but by eddy-current and hysteresis losses in the bearings and motor-generator. As can be seen in Table 7, flywheel energy storage systems today are already competitive with the energy density of batteries, while offering greater service lifetimes in low earth orbit applications. Much of this technology is either already in use or being considered for various applications that are not limited to electric vehicles, backup energy storage, electrical grid power quality and bulk energy storage.

Table 7. NASA GRC Flywheel Technology Metrics and Roadmap.[40]

	Near Term IPACs	Mid Term IPACs	Far Term IPACs
System Energy Density	25 whr/kg	55 whr/kg	75 whr/kg
Charge/Discharge Efficiency	85%	90%	92%
Pulse Power Capacity	40 W/kg	500 W/kg	2000 W/kg
LEO Service Lifetime	15 years	20 years	24 years

As part of a NASA/AFRL program, two counter-rotated flywheels have been integrated as an Integrated Power & Attitude Control System (IPACS) which not only provides energy storage, but also provides attitude control torque through the differential increase and decrease in rotor speed. The technology metrics and future roadmap for the IPACS is listed in and show not only excellent system energy densities and service lifetimes, but also high pulse power capabilities. The high discharge rates provided by flywheels enable pulse power applications including high power pulse radar applications, electrodynamic tethers, MXER tether systems, and the ISEP system. Driven by vehicular and industrial applications, the technologies associated with flywheels is advancing with parallel programs being executed to develop small-scale flywheels for near term technology demonstration flight opportunities to be followed by larger, more capable, reliable flywheels for high-power operational scenarios in the years to come.

II.C. ISEP System Performance

As the ISEP system is fundamentally a form of electric propulsion, it is most useful to compare its performance in terms of propulsion efficiency to other forms of electric propulsion (see Figure 20.) Its performance will be most similar to that of electrodynamic tether systems, with the added benefit that multiple axes of thrust are available for improved control of the thrust angle. The goal of the ISEP system if to provide not only improved performance in terms of propellant utilization (specific impulse I_{sp}) but also in terms of thrust to electrical power ratio (measured here in micro-newtons per watt.)

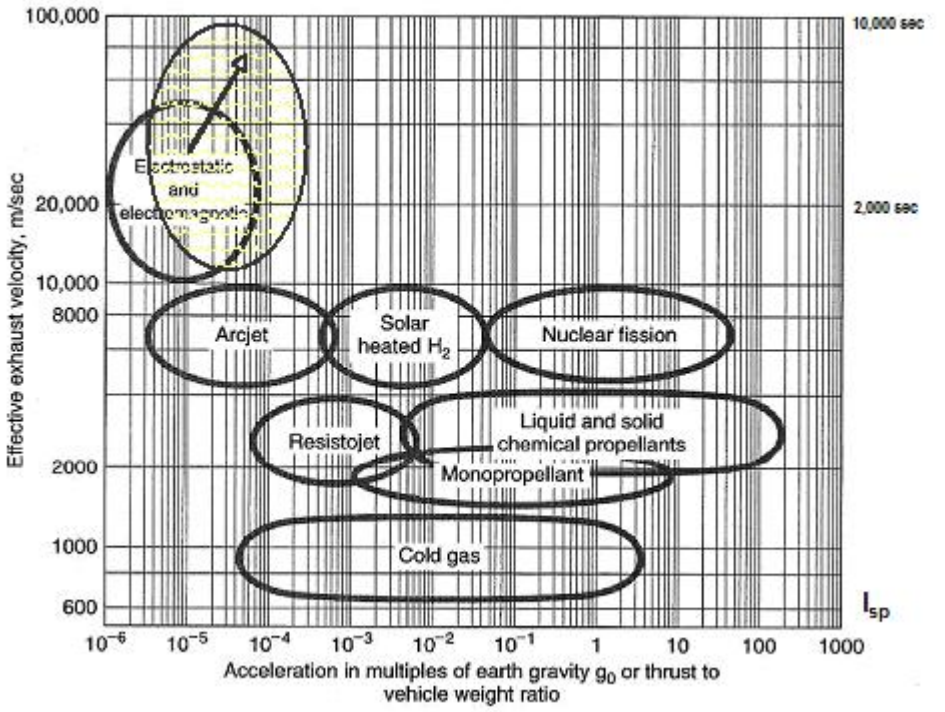

Figure 20. Current landscape of space propulsion technologies (Courtesy Alec Gallimore, U Mich.).

As the basic physical process of ISEP boom propulsion is the same as electrodynamic tether propulsion, it was possible to extend the capabilities of existing tether simulation codes to simulate ISEP systems and analyze their performance. For this effort, the *Te*thered *M*ission *P*lanning and *E*valuation *S*oftware *T*ool (TEMPEST) was used. This code has its origins as a mission simulation and preparation tool for the Tethered Satellite System 1 reflight (TSS-1R) mission that flew on STS-75 in February 1996 and was developed at the University of Michigan by the PI of this effort. This software tool integrates readily available space physics models (see *http://modelweb.gsfc.nasa.gov/*) to predict the geophysical parameters of interest such as the earth's magnetic field (IGRF – International Geomagnetic Reference Field), ionosphere (IRI – International Reference Ionosphere), neutral atmosphere (MSISE – Mass Spectrometer Incoherent Scatter) which then are used to estimate the voltage and currents in bare, insulated, or partially insulated tethers in space. From these currents, the generated thrust is estimated and incorporated in the orbital propagators to estimate the orbital changes that the tethers or in this case ISEP booms can produce.

To determine the performance of the ISEP system in a manner that will enable evaluation of the concept for a variety of mission applications, the performance of the system was estimated over a range of inclinations and altitudes with the booms aligned along the principal axes of the local-vertical/local-horizontal (LVLH) coordinate system. Specifically, the ISEP system with 6 orthogonally aligned 50 meter long booms aligned along the X (along the velocity vector, or "along-track"), Y (the cross-track direction), and Z ("local vertical" or along the radial nadir vector) axes was placed into a series of circular orbits ranging from 300 to 1100 km in altitude at inclinations of 0º, 28.5º, 51.6, 90º, and 97º (approximately sun-synchronous). Each of the three boom axes were then driven with 100 A of current. Based on the survey of plasma contactor technologies summarized in Table 5, we determined that the system would use FEAs to emit electrons at a power lever of 5860 W, and that electron would be collected using hollow cathodes consuming 6480 W of power. The ISEP system was configured to have a total mass of 1000 kilograms with 20 kilograms of hydrogen (as compared to an estimated annual consumption of 6.6kg) fuel for the hollow cathodes, which was consumed at a rate of 280 sccm or 0.20832 mg/sec. The simulations were all started on GMT 012/00:00:00 in 2016, and simulated performance over a period of 30 days, which it was sufficient to determine well converged average performance metrics.

To evaluate the thrust performance of the ISEP system, the 100 ampere current was commanded to flow in the same direction along two of the collinear 50 meter booms, as depicted in Figure 2. To generate torque in the system, 100 ampere currents were commanded to flow in opposite directions along the two collinear 50 meter booms, also as shown in Figure 2. Thrust performance is evaluated as magnitude (N), thrust to power ratio, (μN/W), fuel mass efficiency specific impulse I_{sp}(sec), as well as total ΔV (meters/sec) available after 30 days of continual thrust. Torque performance was evaluated simply in terms of average generated torque (N-m.)

When considering the average available thrust it should be noted that thrust generated by the Z-aligned boom (see Figure 23) is equivalent to that which a gravity gradient 100m long tether would generate, and as is usually the case, thrust levels go down as inclination increases. When considering the LVLH coordinate system, it is obvious that in near-equatorial orbits, the Earth's dipole magnetic field is very closely aligned to the Y axis which accounts for the low thrust levels at low-inclination orbits in Figure 22. As the orbital inclination increase to polar and sun-synchronous (retrograde) the angle between the magnetic field line and the Y-axis boom increases dramatically, which is the source of the spread on sees in the plot. As the thrust-to-power, and specific impulse calculations are fundamentally a function of thrust when available power and fuel consumption are held constant, the results for these two metrics closely resemble the shape and distribution of the average thrust results.

The simulated results indicated that the total ΔV generated by a single boom running at 100A with a 100% duty cycle is in the tens of thousands meters per second range (see Figure 30 through Figure 32.) This provides significant maneuvering capability suitable for long duration missions and those that have large total ΔV requirements.

The magnitudes of the torques generated by the ISEP system by flowing 100 amperes through two collinear boom segments albeit in opposite directions in each are plotted in Figure 36 through Figure 38 for the booms oriented in the X, Y, and Z LVLH directions respectively. As the torque generated by a single boom segment is proportional to $\vec{L} \times \left(i\vec{L} \times \vec{B} \right)$ the unusual shapes of the torque magnitude vs altitude and orbital inclination are due to the geometrical of the

relative orientations of the thrust vector and the moment arm (thrusting boom orientation), with the added presumable effects of the South Atlantic Anomaly (SAA) on the resultant 30 day average available torques. The significant result here is that the ISEP system torque levels are in 1-10 N-m range whereas most of the disturbance torques that concern spacecraft system designers (aerodynamic, gravity gradient, solar pressure, stray magnetic, leaks/outgassing, thermal flex) are in the 10^{-8} to 10^{-1} N-m range, which indicates that the ISEP system has adequate margin to suggest that it can provide the torque needed to afford the control system sufficient attitude control authority.

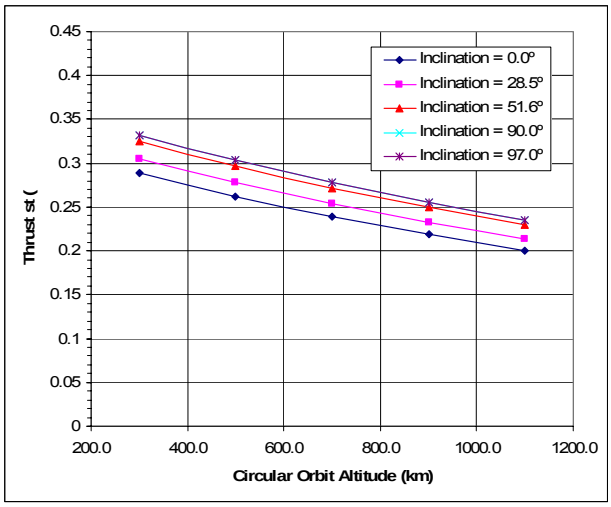

Figure 21. Average thrust magnitude (N) generated by 2x50 meter X-axis (along-track) booms in LEO.

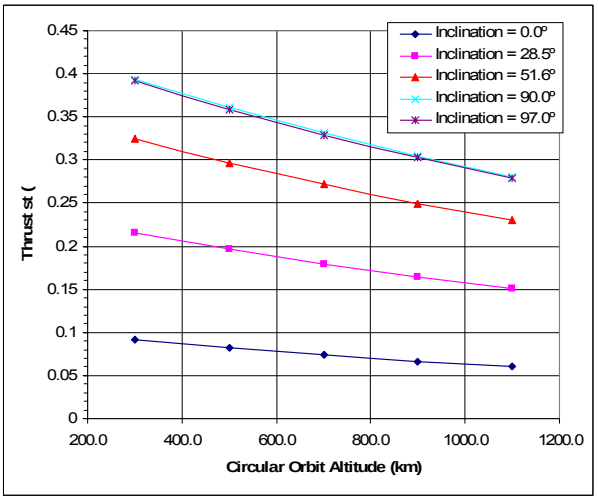

Figure 22. Average thrust magnitude (N) generated by 2x50 meter Y-axis (cross-track) booms in LEO.

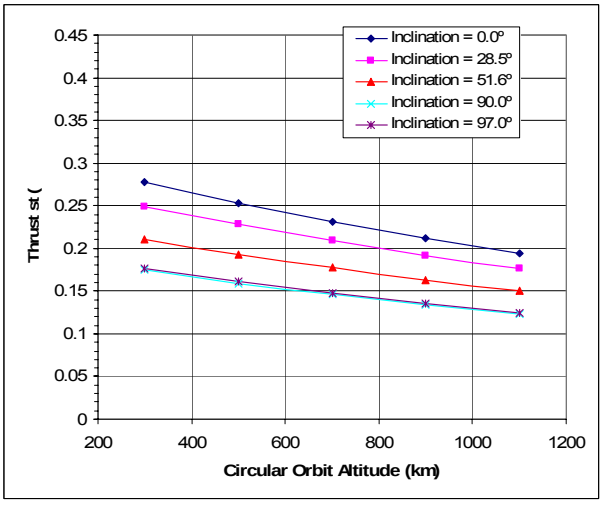

Figure 23. Average thrust magnitude (N) generated by 2x50 meter Z-axis (local vertical) booms in LEO.

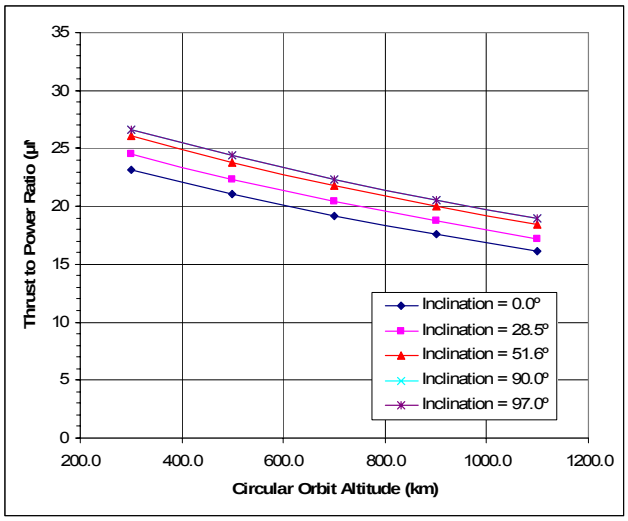

Figure 24. Average thrust-to power ratio (μN/W) for 2x50 meter X-axis (LVLH) booms in LEO.

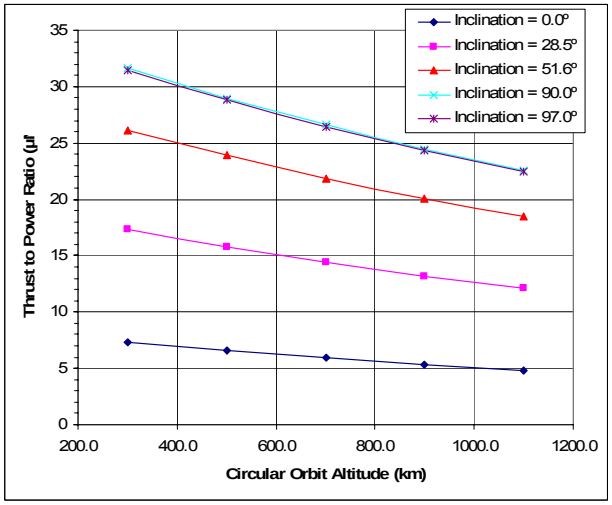

Figure 25. Average thrust-to power ratio (μN/W) for 2x50 meter Y-axis (LVLH) booms in LEO.

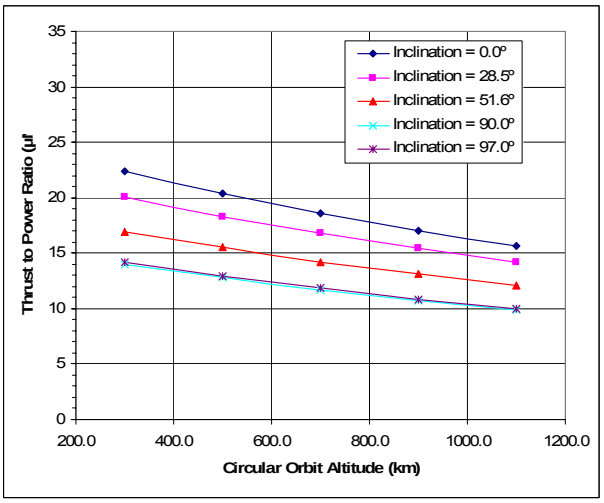

Figure 26. Average thrust-to power ratio (μN/W) for 2x50 meter Z-axis (LVLH) booms in LEO.

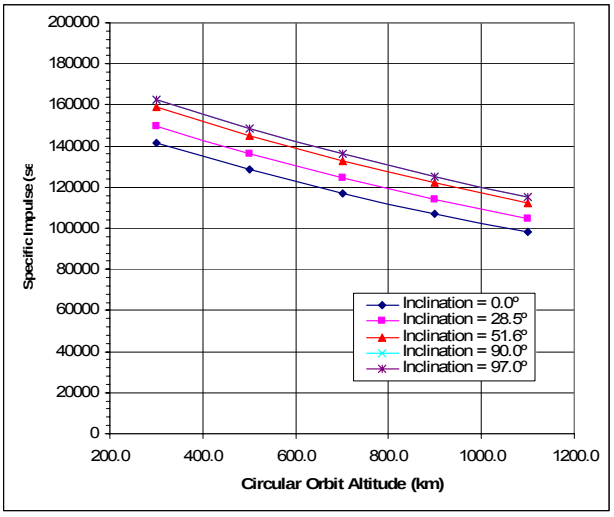

Figure 27. Average specific impulse I_{sp} (sec) for 2x50 meter X-axis (along-track) booms in LEO.

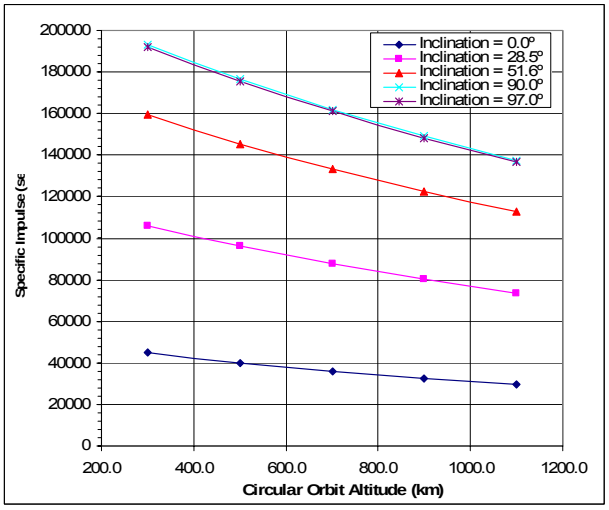

Figure 28. Average specific impulse I_{sp} (sec) for 2x50 meter Y-axis (cross-track) booms in LEO.

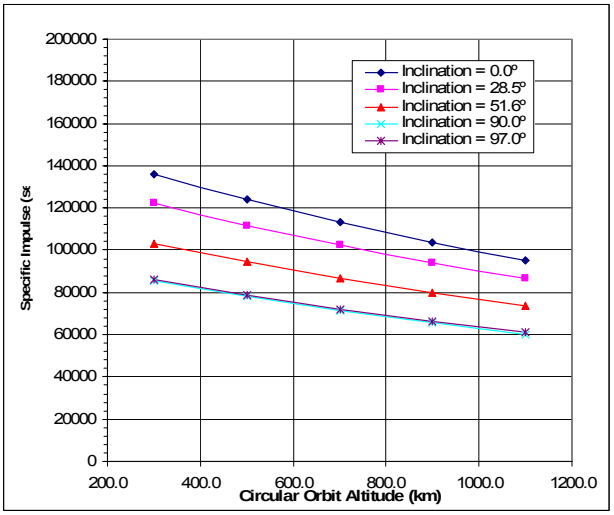

Figure 29. Average specific impulse I_{sp} (sec) for 2x50 meter Z-axis (local vertical) booms in LEO.

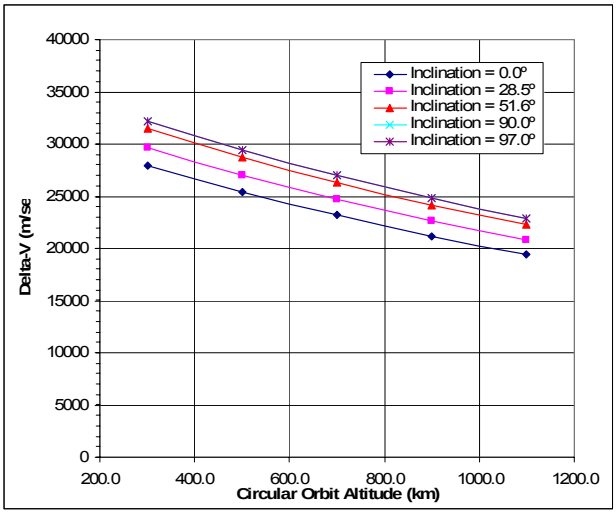

Figure 30. Total ΔV (m/sec) produced by 2x50 meter X-axis (along-track) booms in LEO in a 30 day period of continual thrusting at 100 amperes.

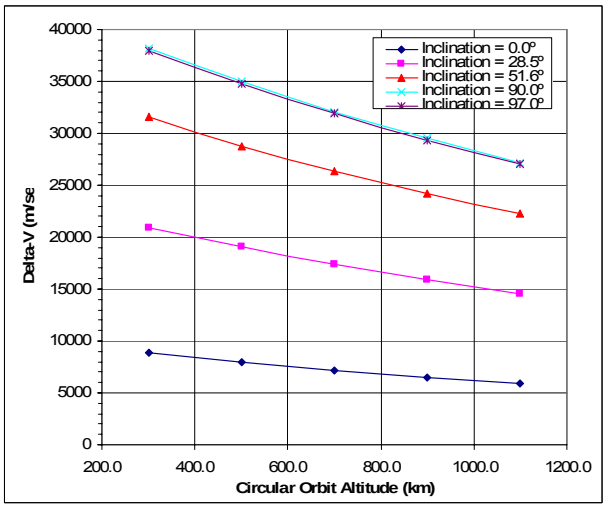

Figure 31. Total ΔV (m/sec) produced by 2x50 meter Y-axis (cross-track) booms in LEO in a 30 day period of continual thrusting at 100 amperes.

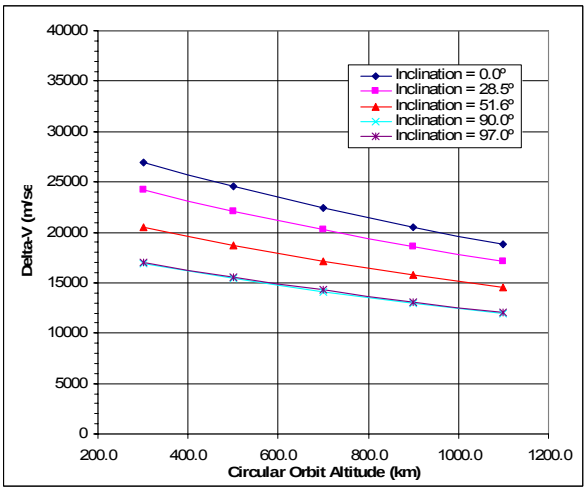

Figure 32. Total ΔV (m/sec) produced by 2x50 meter Z-axis (LVLH) booms in LEO in a 30 day period of continual thrusting at 100 amperes.

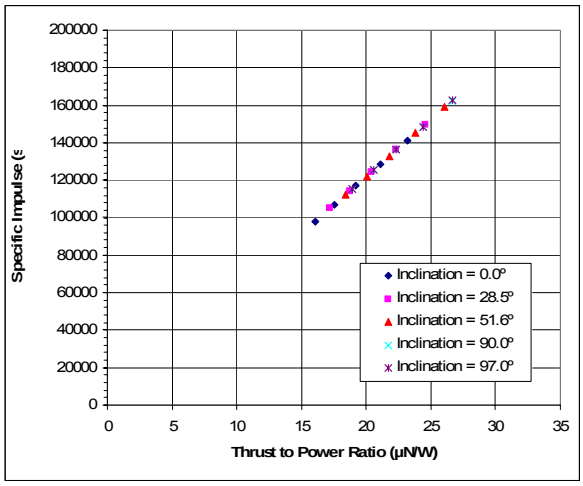

Figure 33. Specific Impulse I_{sp}(sec) vs. thrust-to power ratio (μN/W) for 2x50 meter X-axis (along-track) booms in LEO.

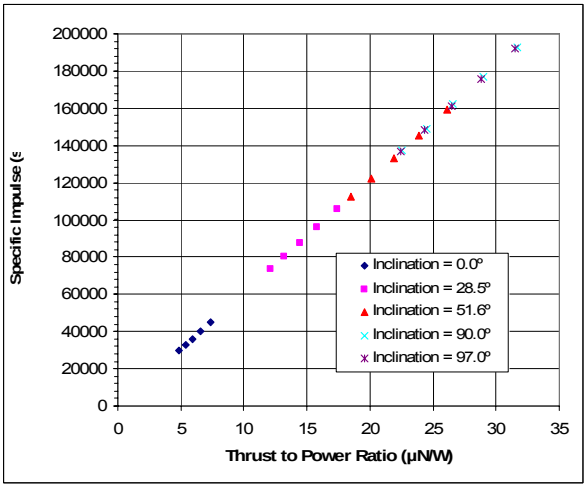

Figure 34. Specific Impulse I_{sp}(sec) vs. thrust-to power ratio (μN/W) for 2x50 meter Y-axis (cross-track) booms in LEO.

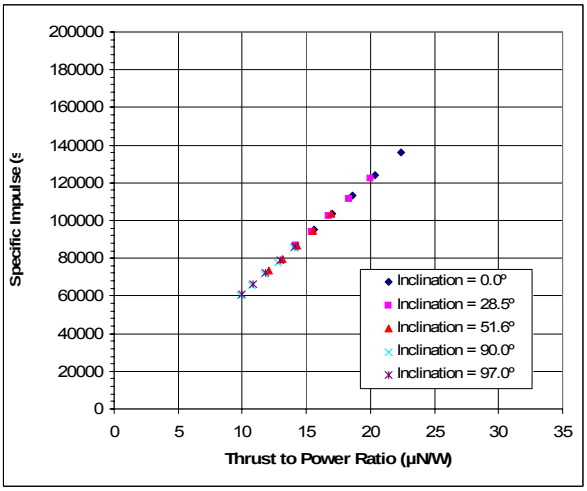

Figure 35. Specific Impulse I_{sp}(sec) vs. thrust-to power ratio (μN/W) for 2x50 meter Z-axis (local vertical) booms in LEO**.**

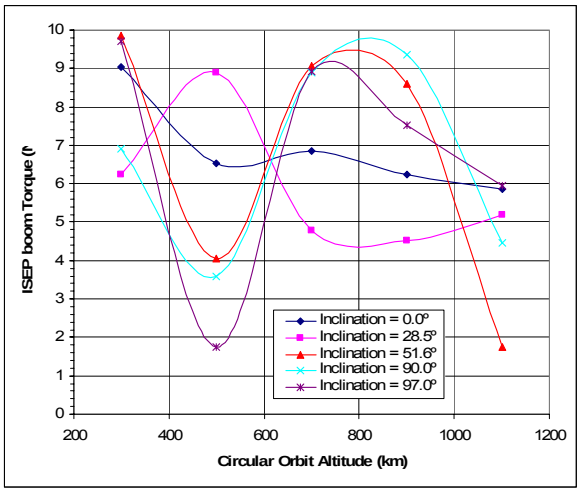

Figure 36. Torque produced (N-m) by opposing 100A currents flowing in 2x50 meter X-axis (LVLH) booms in LEO.

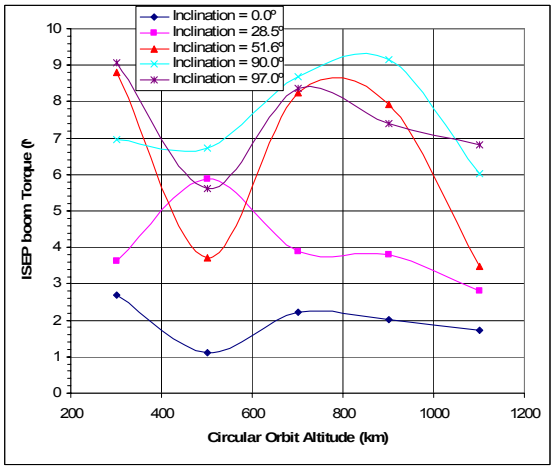

Figure 37. Torque produced (N-m) by opposing 100A currents flowing in 2x50 meter Y-axis (LVLH) booms in LEO.

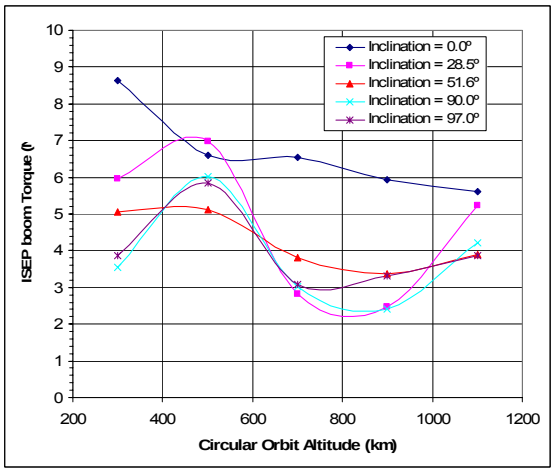

Figure 38. Torque produced (N-m) by opposing 100A currents flowing in 2x50 meter Z-axis (LVLH) booms in LEO.

Because the major source of inefficiency in the electrodynamic propulsion system is in the current collection and emission at the ends of the structure (and not by power dissipated in the boom structure), when multiple ISEP structures are linked in series, the net efficiency of the system increases as more modules are added. This is clearly shown by the near linear increase in specific impulse I_{sp} vs. altitude in Figure 39 when system input power was fixed, and booms of 50 meters, 100 meters, and 200 meters were simulated in a 28.5º inclination orbit. As seen in Figure 40, the thrust-vs.-power and fuel efficiency I_{sp} can be tuned in the ISEP architecture by simply adjusting the length of the booms. In this analysis the mass of conductor is not as critical as the electrodynamic conductor lengths are significantly shorter (10s-100s of meters as compared to 10s-100s of *kilo*meters) therefore represent a small mass fraction of the overall system i contrast to Sorensen's analysis. It should also be noted that the mass of the booms also represents structural elements for end-application use and therefore are not simply a propulsion system mass penalty.

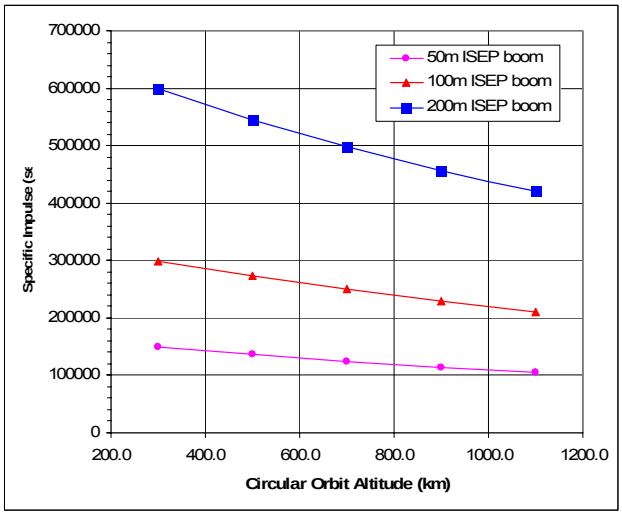

Figure 39. Average specific impulse I_{sp} (sec) for 2x(specified length) meter X-axis (LVLH) booms in a 28.5º inclination LEO.

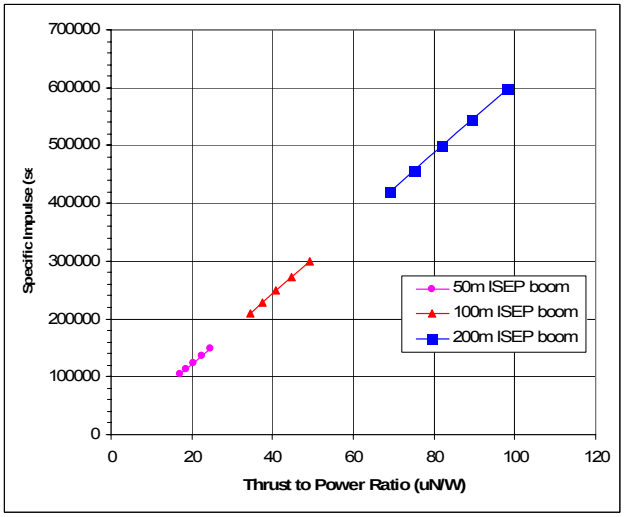

Figure 40. Specific Impulse I_{sp}(sec) vs. thrust-to power ratio (μN/W) for 2x(specified length) meter X-axis (LVLH) booms in a 28.5º inclination LEO.

In conclusion, when the performance of the ISEP system with 50 meter booms is compared in performance to alternate electric propulsions technologies, it represents itself quite favorably as can be seen by the shaded are of Figure 41. The ISEP system can also be compared to an electrodynamic tether system and in particular the MicroSatellite Propellantless Electrodynamic Tether (μPET) system,[41] whose thrust-to-power ratios range from 0.069 to 0.031 N/kW as the orbital inclination varies, however due to the use of a bare tether for electron collection and FEAs for electron emission it is truly propellantless resulting in an infinite I_{sp}. Nevertheless, the ISEP system performance is competitive, and becomes truly interesting where modular structural elements are needed for the mission, and even more so where multiple boom elements can be collinearly assembled.

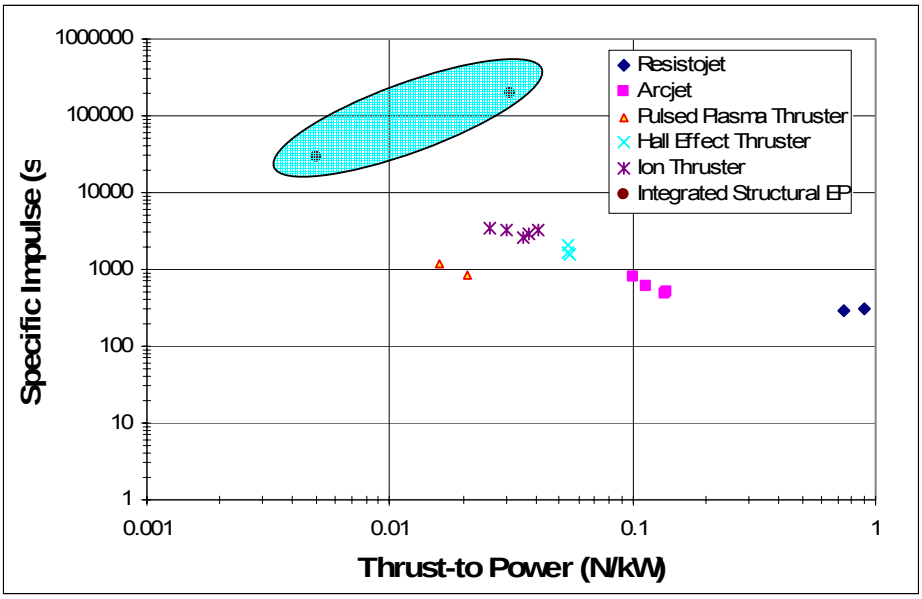

Figure 41. Comparison of ISEP performance with respect to other electric propulsion technologies[42].

II.D. TECHNOLOGY DEMONSTRATION CONCEPT DESIGN

As we discussed in Section I.D.2, although there are several technical challenges that must be addressed to advance the technology readiness level of the ISEP concept to the point where it can be used in operational space systems, most of the core required technologies are common with other space systems and are receiving significant attention and investment by other NASA and DoD efforts. The one key challenge that is relatively unique to the ISEP concept is the requirement for a power- and mass-efficient means for collecting and transmitting large currents between the ISEP structure and the ambient space plasma. To address this technical challenge, we have developed a concept design for an experiment that can be accomplished within the scope of a Phase II NIAC effort. The purpose of this experiment will be to establish the feasibility of generating significant electrodynamic forces using a structural element with integrated conductive elements.

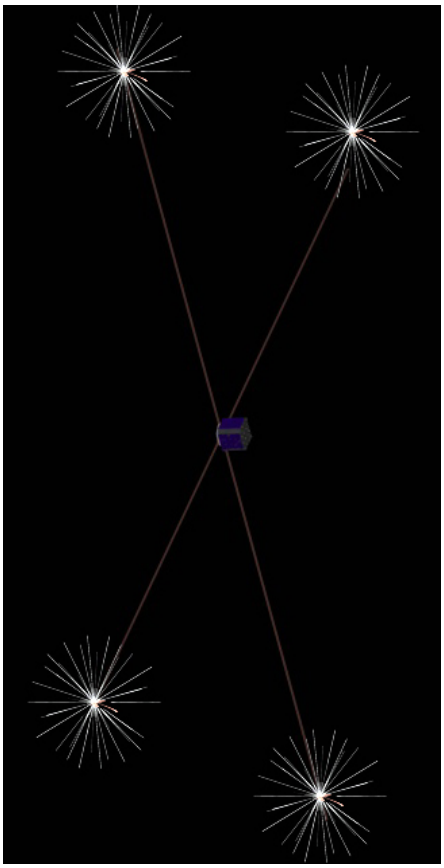

Figure 42. Nanosatellite experiment carrying a number of Field Emissive Arrays and 4 rigid insulated booms with electron collecting spheres at their ends.

II.D.1 Experiment Objectives

The key technical objectives of the Phase II experiment effort will be to:

- Test the performance of a candidate propellantless plasma contactor technology;
- Demonstrate that meaningful thrust and torque levels can be generated using relatively short (few meters) electrodynamic element;

The data obtained on plasma contactor performance and electrodynamic thrust will validate the feasibility of the ISEP concept, and provide crucial guidance on how to design future space systems incorporating structures with integrated electrodynamic propulsion.

II.D.2 Experiment Concept

In developing the proposed experiment concept, we considered both ground-based and space-based experiments. Due to the complexity and cost of matching the many critical parameters of an ISEP space system in a ground-based vacuum chamber experiment, such as length scales, plasma densities, ultra-high-vacuum and cleanliness requirements, and millinewton-level thrust sensitivities, we came to the conclusion that within the scope of a Phase II NIAC effort we could best advance the ISEP technology by conducting a very simple flight experiment. To accomplish this flight experiment within the funding scope of a NIAC Phase II effort, we will perform the experiment utilizing the low-cost CubeSat nanosatellite platform. By taking advantage of the low launch costs available through the University CubeSat platform ($40K/cubesat), and re-using nanosatellite component technologies we have already developed for our upcoming "Multi-Application Survivable Tether" (MAST) nanosatellite experiment,[43] a simple flight demonstration can be performed within the funding scope of a Phase II effort.

II.D.2.i CubeSat Program Background

Figure 46. P-POD Deployer that holds 3 CubeSats (left), and a representative CubeSat (right).

The development of satellites, spacecraft subsystems and components is still dominated by the launch problem – the availability of frequent, low-cost launch opportunities. Often, spacecraft developers target secondary launch opportunities for their experiments and technology demonstrators, and a number of nanosatellite payload standards have evolved. The most popular one is that of the CubeSat (http://www.cubesat.org) – a 10x10x10 cm spacecraft with mass of no more than 1-kilogram. This standard is quite interesting in that there is typically at least one launch opportunity per year for CubeSat satellites through the University Cubesat program coordinated by California Polytechnic University at San Luis Obispo. Through this program, experiments can be launched at a cost of $40,000 per CubeSat. While this is not cost competitive with other launch vehicles on a per-kilogram basis, the charge includes integration, licensing and launch costs, making it cost-effective for small, simple experiments.

Over the past three years, TUI has been an active participant in the CubeSat community, and on April 21, 2006 we signed a Memorandum of Agreement with CalPoly for launch of the three nanosatellites which comprise our MAST experiment in August of 2006. The MAST experiment will deploy a 1-km long survivable tether structure between two nanosatellites, and a third nanosatellite will slowly crawl up and down the CubeSats, inspecting the tether to determine its ability to withstand degradation by orbital debris and micrometeorites. Pictures of the MAST nanosatellites taken during the assembly process are shown in Figure 44 and Figure 45.

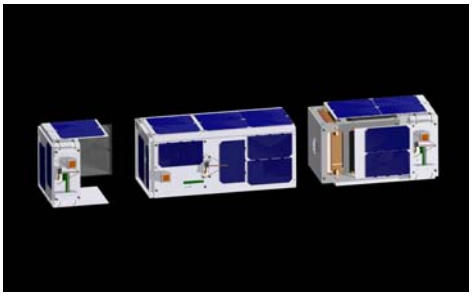

Figure 43. The MAST nanosatellites.

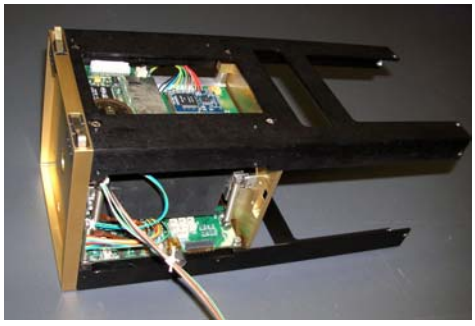

Figure 44. The MAST tether inspector nanosatellite in final assembly (13Apr06).

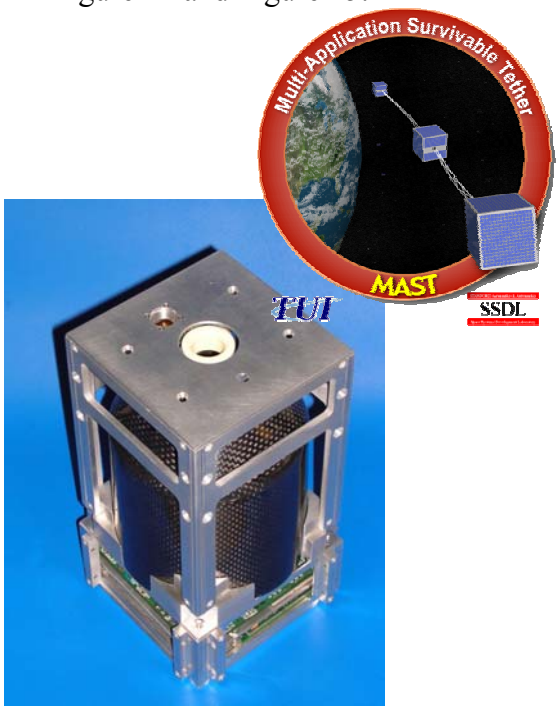

Figure 45. The MAST tether deployer nanosat in preliminary assembly.

II.D.3 Experiment Details

The proposed ISEP experiment will deploy several lightweight conducting boom structures, 5-10 m in length, from a nanosatellite bus, as illustrated in Figure 47, and demonstrate generation of electrodynamic thrust and torque by driving currents along these booms. To demonstrate emission of electrons to the space plasma without the use of propellant or consumables, we will use a combination of field emissive array cathodes (FEACs) along with simple lightweight, compact electron collectors to drive up to 1 ampere of current through the booms. The goal is to generate current flow through the rigid conductors in such a way as to produce measurable thrust and torque on the host spacecraft, further validating the proposed concept.

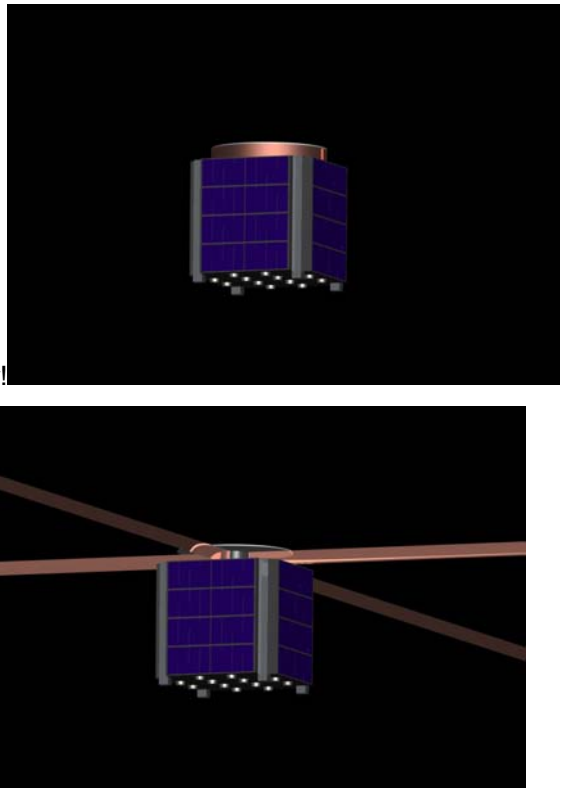

Error!

Figure 47. Concept for an ISEP CubeSat-class nanosatellite (10x10x10 cm, 1kg) experiment. (TOP) pre-launch stowed configuration (BOTTOM) with the four booms deployed. The FEACs are located on the bottom face.

Low-Cost/High-Risk Approach

In order to accomplish the experiment within the funding scope of a Phase II effort, the experiment will be designed and conducted as a class-D mission, with single-string design and minimal ground testing. In doing so, we will necessarily be accepting a significant level of mission risk; however, the costs associated with conducting extensive ground testing of the technology prior to the flight are significantly greater than the $40K launch costs, so this approach makes sense from a cost-risk perspective.

System Concept

The experiment concept design seeks to balance the extreme limitations in mass, volume, and cost with the objective to demonstrate the generation of significant levels of thrust and torque using short electrodynamic elements. The primary limitation on this experiment boils down to the small amount of real-estate available for body-mounted solar cells. When all of the faces of a 10x10x10 cm CubeSat are covered with readily available triple-junction solar cells, the average available power to the spacecraft systems is on the order of 1 watt. For this experiment to produce thrust and torque levels that will be of interest for future applications and demonstrate high-current operation of propellantless plasma contactor technologies, it must drive currents in the range of 0.5-1 Amperes along its booms. To achieve these current levels within such a power-limited system,

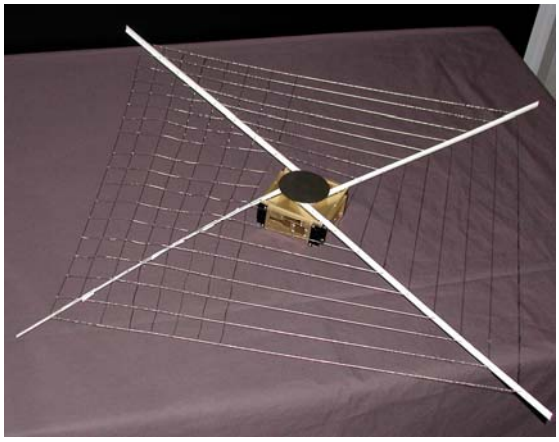

Figure 48. Photo of a 5x10x10 cm TUI nanosat with a grid rectenna prototype deployed using four booms stowed and deployed in a manner similar to the proposed ISEP experiment.

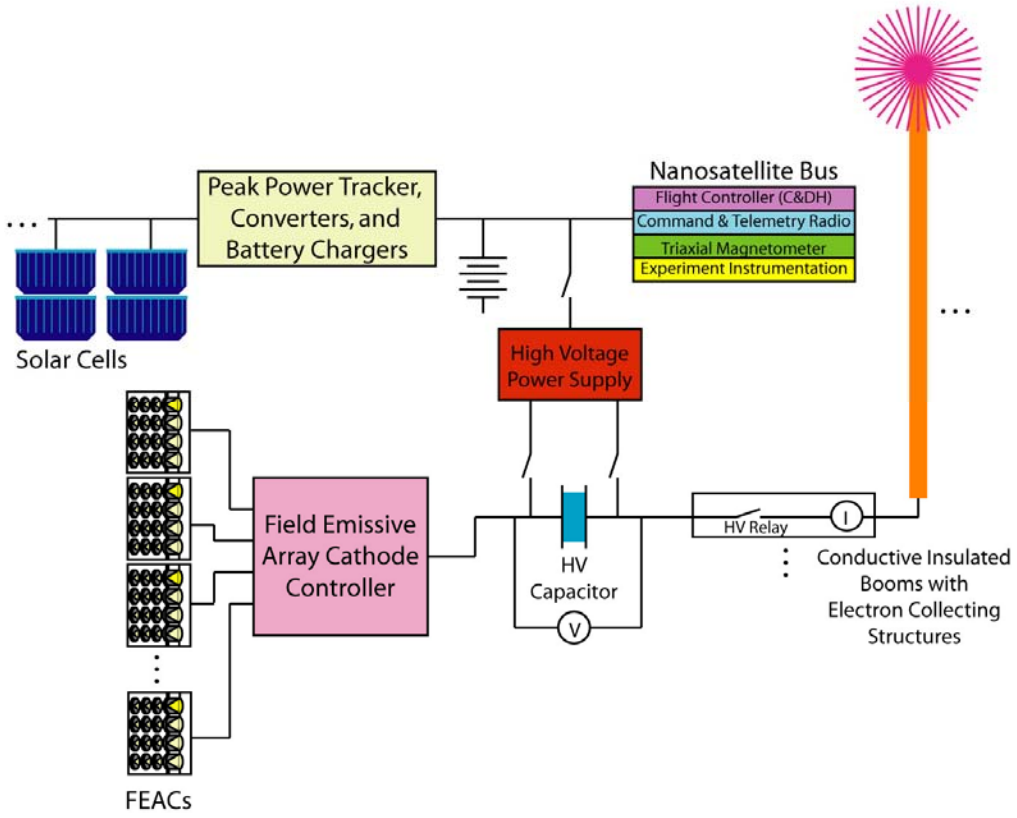

Figure 49. Block diagram of the proposed ISEP nanosatellite experiment. In this diagram a single boom with electron collection sphere is depicted, however additional booms with connecting relay and current monitor can be readily added.

the experiment will operate in a pulsed mode, with the ISEP system driven for periods on the order of 0.1 to 1 seconds every several hours.

A block diagram of the experiment concept is shown in Figure 49. Body mounted solar cells will be used to collect energy, which will be used both to drive the nanosatellite bus systems and charge up a high voltage capacitor. When the capacitor is fully charged, a high-voltage relay will be fired to allow the capacitor to drive current along the deployed conductive booms. At the distal end of the boom, a simple passive contactor with extremely high surface-area-to-mass will be used to collect electrons from the ambient plasma. These electrons will flow along the boom to the Cubesat, where a bank of FEAC devices mounted on one of the six faces of the cube will eject them back into the ambient plasma. The number of FEACs and the size of the passive collector will be chosen to enable currents of up to 1 Amp to be driven through this system. By energizing various combinations of the four booms, we will demonstrate both net thrust and net torque on the cubesat. A combination of magnetometers and MEMS-based accelerometers and gyros will be used to sense changes in the satellite's state after each current pulse. The timing and direction of the current pulses will be chosen to demonstrate active control over the cubesat's attitude, such as by first removing any initial tumble due to ejection from the PPOD or deployment of the booms, and then spinning up the system in a controllable manner.

In the following paragraphs we detail the baseline technology concepts for the boom, electron emitter, and electron collector components of the ISEP nanosatellite experiment.

Deployable Conducting Booms

To achieve separation between the electron emitters and the electron collector, a rigid conductive boom will be used as previously discussed in the ISEP system. On the nanosatellite scale, we propose to baseline the use of spring steel (measureing tape) or copper beryllium strips as they have appropriate stiffness, mass and packing density for this scale of boom. Figure 48 shows a photo of a proof-of-concept prototype of a grid rectenna deployed from a TUI nanosatellite using a similar assemblage of spring steel booms. While the illustration in Figure 46 shows four 5-m booms, during the preliminary design phase of this experiment, a trade study will be performed to determine the optimal boom length to ensure that the sheaths from electron collection and emission do not overlap. Then, based on the available mass and volume, the number of booms may be decreased to allow for the booms to be lengthened.

Propellantless Electron Emission

To accomplish electron emission without the use of consumables, we intend to utilize SRI International's Spindt field emissive array emissive cathodes (FEACs) mounted on one face of the CubeSat body. TUI has been working with SRI for a number of years and has experience with chamber testing of the SRI FEACs in support of electrodynamic tether missions. TUI already has over 20 of these devices available in-house, which are available for integration and into a nanosatellite flight experiment. As has been mentioned previously, there are handling and integration issues that deal with the cleanliness and contamination of the tips that would severely and adversely affect their performance in flight. In addition to proper handling, sealing and conditioning of these cathodes in flight, additional margin is gained through the integration of a number of multiple cathodes onto a single face of the nanosatellite so that should one device fail, redundant devices could then be utilized. Currently TUI is collaborating with SRI under DARPA funding on an interface specification for use of FEACs with space tether systems, and are negotiating the availability of SRI's FEAC drive electronics in support of this nanosatellite experiment.

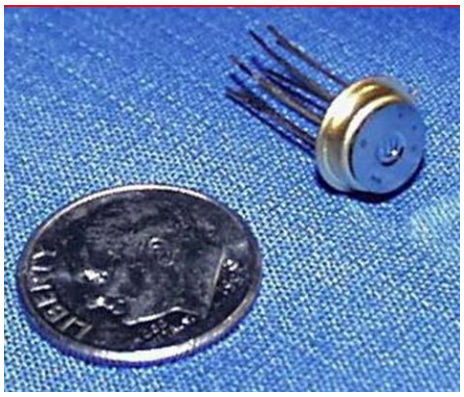

Figure 50. SRI's Spindt type FEAC with 50,000 tips packaged in a standard

Electron Collection: The "Hedgehog" Contactor

Although our analyses indicate that an operational ISEP system will be most effective if it utilizes a hollow cathode plasma contactor to perform active collection of electrons at the anode end of the system, hollow cathode devices require mass, power, and propellant well in excess of what can be supported in a nanosatellite experiment. Passive collection of electrons using a large surface area conductor such as an conducting sphere or a gridded mesh sphere[44] deployed by inflation of a UV-dissolving membrane have been proposed for the MXER tether system; however solid sphere or gridsphere collectors would also require a significant fraction of the available nanosatellite resources. To enable the ISEP nanosatellite to perform passive electron collection with a large effective collecting area yet with minimal mass and volume requirements, we propose to utilize a novel electron collection method called the "Hedgehog", illustrated in Figure 52. This device is simply a bundle of conductive yarns, such as metal-coated aramid fibers such as Aracon® or AmberStrand®, which will be tied at one end to the distal end of the boom. These yarns will be left untwisted, so that when they are charged to even relatively small

voltages, the individual fibers in the yarns will spread apart due to electrostatic repulsion, forming a roughly spherical "Koosh-ball" like structure. The concept originated from observations made during our efforts to braid tether structures using AmberStrand yarn, where we found that untwisted segments of the yarn tend to spead apart and become almost unmanageable just due to electrostatic charges accumulated during handling. A 2 meter diameter 'Hedgehog' structure with a conductive yarn every 40º of solid angle, and a 12 micron filament approximately every 1º of solid angle will have an estimated mass of 10 grams. A simple proof-of-concept experiment was conducted in which a few strands of Aracon® yarn were threaded through a punched segment of copper beryllium tape, and electrically connected to the top of a Van de Graaf generator. In Figure 51 we can readily see how the few yarns align themselves when the generator is turned on even in the presence of Earth's gravity. In zero-gee, it is expected that the effect of the electrostatic forces will be more pronounced and symmetric. Preliminary analyses indicate that this structure can potentially collect over 90% of the electron current that a similarly sized inflatable conducting sphere would collect, with a much lower total system mass.

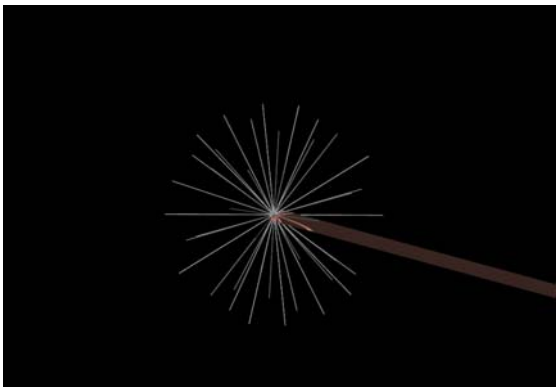

Figure 52. Electron collector at the end of the boom constructed of electrostatically separated conductive elements.

To enable the system to emit currents in the 100s of milliamperes range, the potential drop across the entire system ranging from the electron collection structure, drop along the boom(s) and acceleration potential of the FEAs, will be in the 500-1000 volt range. The instrumentation aboard the spacecraft will be used to measure the amount of current actually flowing through the spacecraft boom(s), tip and gate currents from the FEACs, ambient magnetic field to estimate the thrust levels as well as vehicle orientation. By comparing the measured ambient magnetic field with the Earth's modeled field using such models as IGRF or the WMM (knowing the spacecrafts position in space), the vehicle's attitude and can be estimated to within a few degrees. When the system has been pumped up to affect spacecraft rotation at the rate of a few rotations per orbit, the magnetometer-derived attitude can be used to estimate vehicle spin rates

Figure 51. Simple Aracon® structure demonstrating the dispersion and tensioning of the elements due to the charging of the elements by a Van de Graaf generator.

as well.

II.D.4 Concept of operations

In summary, the mission operations of the proposed nanosatellite experiment will be as follows:

1. After the third stage delivers its primary payload to orbit, the P-POD deploys the nanosatellite experiment.
2. After allowing sufficient time to elapse to ensure physical separation from its neighbors, a burn wire is activated to release the booms.
3. The spacecraft assumes a low-power configuration in order to maximize the transfer of incident solar radiation to the energy storage capacitor. Preliminary calculations suggest that the average available 1W from the spacecraft's solar panels would allow the capacitor to be charged in 4-6 orbital periods.
4. Once residual dynamics from boom deployment have dampened, and sufficient charge levels have been achieved, the spacecraft monitors the strength and orientation of the ambient magnetic field and the day/night status of its orbital position. When the spacecraft is appropriately aligned to generate a force/torque in the desired direction and when the spacecraft is preferable illuminated (the ambient plasma density is typically higher in the daytime allowing for increased electron collection, and reduced space charge limiting effects), the following steps are executed in short order:
    a. The high voltage power supply (HVPS) is disconnected from the energy storage capacitor.
    b. Appropriate high voltage relays are closed between the capacitor and the desired booms.
    c. The FEAs are commanded to emit current, thereby closing the circuit and effecting the discharge of the energy storage capacitor. During the discharge, high speed sampling of the capacitor voltage, boom currents, and magnetic field (for orientation) is enabled.
    d. Once the capacitor has been discharged, the FEA are disabled, the HV relays to the boom(s) are opened, and if there is sufficient battery power, the HVPS is energized once again to initiate charging of the energy storage capacitor.

The criteria for mission success include the efficient emission of electrons to space plasma, with torque inducing currents flowing through the spacecraft booms, affecting a measurable increase in the rotational rate of the spacecraft. It is estimated that a few weeks of mission operations which will most likely be pre-programmed and autonomous to reduce overall costs are sufficient to achieve the aforementioned mission objectives. In addition to receiving spacecraft telemetry via RF downlink, it is expected that with suitable placement of reflective materials on the spacecraft and boom(s), both passive observers and laser tracking stations should be able to directly observe the rotation of this nanosatellite.

The proposed low-cost nanosatellite experiment not only demonstrates the advancement of a key technology of the ISEP system and architecture but also of a key technology for any electrodynamic tether mission, especially one where the tether system needs to be spinning. The success of this mission will also demonstrate the feasibility and practicality of performing

significant, simple, low-cost spaceflight experiments within the confines of a Phase II NIAC effort, which is similar in duration and funds of a NASA Phase II SBIR/STTR effort. While a number of nanosatellites and CubeSats have been developed and flown to date, the goals of most of these missions was to demonstrate technologies associated with nanosatellite bus components and technologies. TUI is suggesting a new paradigm by which program relevant, important small experiments can be designed, fabricated, and launched within the confines of a Phase II program such as is being done with the Multi-Application Survivable Tether (MAST) experiment[45] which was developed as part of a NASA Phase II STTR and is scheduled to be launched in August 2006. The MAST experiment is a scaled demonstration and quantification of the survivability of the Momentum Exchange Electrodynamic Reboost (MXER) system which was initially funded as a NIAC concept in 1999.

The proposed experiment's goal is not only to perform a meaningful experiment to validate technologies and reduce risks associated with the ISEP system, but to also inspire and motivate others to expand their vision to include the possibility of doing simple experiments in space within the confines of NIAC and NASA Phase II innovative research programs.

III. CONCLUSIONS

This Phase I effort has demonstrated the feasibility of an innovative multifunctional propulsion-and-structure system concept, called the Integrated Structural Electrodynamic Propulsion (ISEP), which uses current-carrying booms deployed from a spacecraft to generate thrust with little or no expenditure of fuel. This system and architecture is based on multiple modular elements consisting of booms and nodes that can be self-assembled into larger space structures with integrated propulsion which can then be used directly in support of NASA's Vision for Space Exploration (VSE) or any other missions that require significant ΔV to achieve their mission objective. Trade studies and technology assessments have concluded that there are no fundamental issues that would prevent the design and construction of an ISEP system in the relatively near future. Nevertheless, significant engineering challenges remain, most notably with the plasma contacts to affect current closure. To advance the state of the art and mitigate the risks associated with propellantless propulsion and electron emission in particular, TUI designed a nanosatellite space flight experiment that can be fabricated and flown within the constructs of a Phase II NIAC effort.

Simulation results conclude that the ISEP system is competitive with other electric propulsion technologies as a single node with a single set of booms. Although a single ISEP element can provide useful propulsion, this architectural approach really pays off when two or more elements are combined to create a larger structure with commensurate increases in thrust and system efficiency.

The ISEP system bridges the gap between traditional electric propulsion and electrodynamic tethers offering highly efficient propulsion with the added benefit of structural members at the expense of a small quantity of fuel for the plasma contactors to actively collect and emit electrons. For the VSE, the ISEP system could greatly reduce the overall costs of the exploration of space and thus could enable the Vision to evolve into an economically sustainable long-term development of the Moon and near-Earth space.

IV. APPENDIX A - OCTOBER 2005 ANNUAL MEETING POSTER

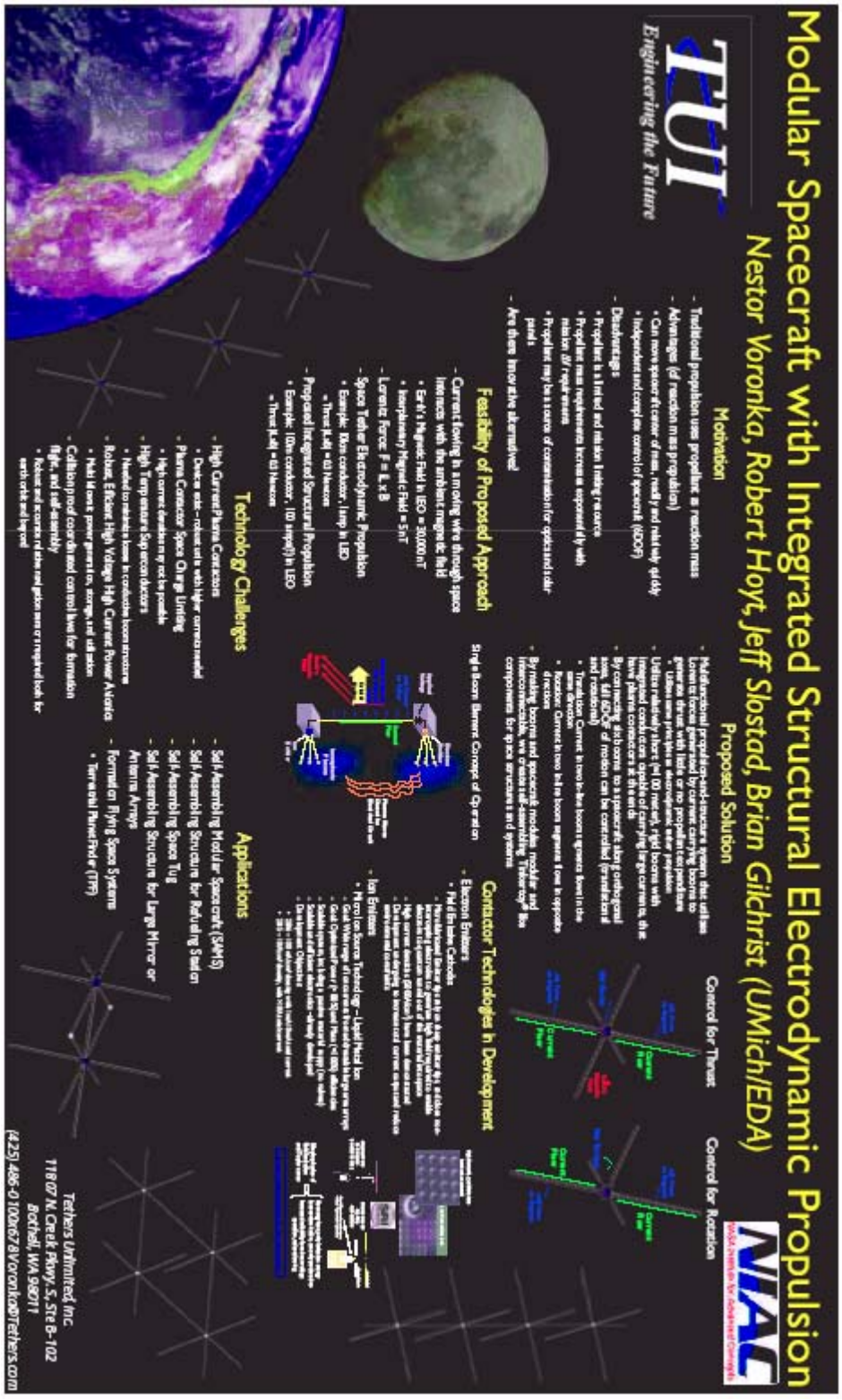

V. REFERENCES

1. Hoyt, R.P., Uphoff, C.W., "Cislunar Tether Transport System", AIAA Paper 99-2690, *35th Joint Propulsion Conference*, June 1999.

2 Drell, SD, Foley, HM, Ruderman, MA, "Drag and Propulsion of Large Satellites in the Ionosphere: An Alfvén Engine in Space," *J. Geophys. Res.*, Vol. 70, No. 13, 7/1/65, pp. 3131-3146.

3 Thompson, D.C., C. Bonifazi, B.E. Gilchrist, S.D. Williams, W.J. Raitt, J.-P. Lebreton, and W.J. Burke, "The Current-Voltage Characteristics of a Large Probe in Low Earth Orbit: TSS-1R Results," Geophys. Res. Lett.,Vol. 25 , No. 4, p. 415-418, 1998.

4 L. Johnson, B. Gilchrist, E. Lorenzini, N. Stone, K. Wright, "Propulsive Small Expendable Deployer System (ProSEDS) Experiment: Mission Overview & Status," AIAA-2003-5094, 39th AIAA/ASME/SAE/ASEE Joint Propulsion Conference and Exhibit, Huntsville, Alabama, July 20-23, 2003.

5 Gilchrist, B. E., K.L. Jensen, A.D. Gallimore, J. Severns, Space Based Applications For FEA Cathodes (FEACs), Materials Issues in Vacuum Microelectronics: Symposium Proceedings, Materials Research Society, Warrendale, PA, 2000.

6 Hoyt, R.P, Voronka, N.R., Slostad, J.T., "Microsatellite Propoellantless Electrodynamic Tether Propulsion System." July 2004, JANNAF, Las Vegas, NV.

7 Hoyt, R.P., Slostad, J.T., Frank, S.S., "A Modular Momentum-Exchange/Electrodynamic-Reboost Tether System Architecture," AIAA Paper 2003-5214, *39th Joint Propulsion Conference*, Huntsville, AL, July 2003.

8 Sorensen, K., "Optimal ED Tether for MXER", Memorandum Dated 25 Aug 04.

[9] Hopkins, R.G. "Long-Access Orbits." The Aerospace Corporation briefing presentation.

10. Vas, I., Kelly, T.J., Scarl, E.A, "Space station reboost with electrodynamic tethers," *J. Spacecraft & Rockets*, 37(2) Mar 2000, p 154-164.

11. Wertz, J., Larson, W., "Space Mission Analysis and Design," Microcosm Press, 3rd Edition, 1999.

12. Callihan, R., "Fed-Up with the High Price of Copper – Copper Clad Aluminum is the Answer," Commscope Bimetals White Paper.

13. Gilchrist, B. E., C. Bonifazi, S. G. Bilén, W.J. Raitt, W. J. Burke, N. H. Stone, J. P. Lebreton, "Enhanced electrodynamic tether currents due to electron emission from a neutral gas discharge: Results from the TSS-1R mission," Geophys. Res. Lett.,Vol. 25 , No. 4, p. 437-440, 1998.

14 Tomczak S.J., et. al., "Properties and Improved Space Survivability of POSS Polyimides," Mater. Res. Soc. Symp. Proc. Vol. 851, 2005.

15 Kern, O., Bilén, S.G., "Model of Current Collection to Small Breaches in Electrodynamic-Tether Insulation," AIAA Paper 2003-4947, 39th JPC, Huntsville, AL, 20-23 July 2003.

16 Murphey, Tomas, "Booms and Trusses", Recent Advances in Gossamer Spacecraft, Jenkins, Christopher, ed., Progress in Astronautics and Aeronautics, vol. 212, AIAA, 2006, pp. 1-43.

17. Murphy, D., Eskenazi, M., White, S., Spence, B. "Thin-film and Crystalline Solar Cell Array System Performance Calculations," 29th Photovoltaic Specialist Conference, IEEE, May 2000, pp. 782-787.

18 Greshik, G., Mikulas, M., “Design Study of a Square Solar Sail Architecture,” 42nd AIAA Structures, Structural Dynamics, and Materials Conference, AIAA Paper 2001-1259, April 2001.

19 Beal, B., Grys, K., and Welander, B., "Development of a High Current Hollow Cathode for high Power Hall Thrusters," Joint Army Navy NASA Air Force Propulsion Meeting/Liquid Propulsion Subcommittee/Spacecraft Propulsion Subcommittee Conference, 2005, pp. 1-8.

20 Brophy, J.R., and Garner, C.E., "Tests of High Current Hollow Cathodes for Ion Engines," AIAA/ASME/SAE/ASEE 24th Joint Propulsion Conference, AIAA, 1988, pp. 1-11.

21 Carpenter, C.B., and Patterson, M.J., "High-Current Hollow Cathode Development," 2001 International Electric Propulsion Conference, 2001, pp. 1-8.

22 Goebel, D.M., and Watkins, R.M., "High current, low pressure plasma cathode electron gun," Review of Scientific Instruments, Vol. 71, No. 2, 2000, pp. 1-11.

23 Gomer, R., "Field emission," Vol. 2005, No. July 1, 2002, pp. 2.

24 Spindt, Charles A. (Capp), Brodie, I, Holland, C., Schwoebel, P., “Spindt Field Emitter Arrays”, Vacuum Microelectronics, ed.,Wei Zhu, October 2001.

25 Dekker, A.J., "Thermionic Emission," Vol. 2004, No. 5 / 3, 2002, pp. 2.

26 Bonifazi, C., Svelto, F., and Sabbagh, J., "TSS Core Equipment I - Electrodynamic Package and Rational for System Electrodynamic Analysis," Il Nuovo Cimento Della Societa Italiana Di Fisica, Vol. 17C, No. 1, 1994, pp. 13-47.

27 Dobrowolny, M., and Stone, N.H., "A Technical Overview of TSS-1: the First Tethered-Satellite System Mission," Il Nuovo Cimento Della Societa Italiana Di Fisica, Vol. 17C, No. 1, 1994, pp. 1-12.

28 Parker, L.W., and Murphy, B.B., "Potential Buildup on an Electron-Emitting Ionospheric Satellite," Journal of Goephysical Research, Vol. 72, No. 5, 1967, pp. 1631-1636.

29 Thompson, D.C., Bonifazi, C., and Gilchrist, B.E., "The current-voltage characteristics of a large probe in low Earth orbit: TSS-1R results," Geophysical Research Letters, Vol. 25, No. 4, 1998, pp. 413-416.

30 Stone, N.H., and Moore, J.D., "Grid Sphere Electrodes used for Current Collection at the Positive Pole of Electrodynamic Tethers," 45th AIAA/ASME/ASCE/AHS/ASC Structures, Structural Dynamics & Materials Conference, AIAA, 2004, pp. 1-7.

31 Lieberman, M.A., and Lichtenberg, A.J., "Principles of Plasma Discharges and Materials Processing," Wiley-Interscience, Hoboken, NJ, 2005, pp. 757.

32 Parker, L.W., "Plasmasheath-Photosheath theory for Large High-Voltage Space Structures," edited by H.B. Garrett and C.P. Pike, Space Systems and their Interactions with the Earth's Space Environment, AIAA Press, 1980, pp. 477-491.

33 Hutchinson, I.H., "Principles of Plasma Diagnostics," Cambridge University Press, Cambridge, United Kingdom, 2002, pp. 440.

34 Luginsland, J.W., McGee, S., and Lau, Y.Y., "Virtual Cathode Formation Due to Electromagnetic Transients," IEEE Transactions on Plasma Science, Vol. 26, No. 3, 1998, pp. 901-904.

35 Humphries, S.J., "Charged Particle Beams," John Wiley & Sons, Inc., New York, 1990, pp. 834.

36 Lau, Y.Y., "Simple Theory for the Two-Dimensional Child-Langmuir Law," Physical Review Letters, Vol. 87, No. 27, 2001, pp. 278301/1-278301/3.

[37] Morris, David P., "Optimizing Space-Charge Limits of Electron Emission Into Plasmas With Application to In-Space Electric Propulsion." PhD Thesis, University of Michigan, 2005.

[38] Morris, D., Gilchrist, B., Gallimore, A., "Applications of Dual Grids to Cold Cathode/Field Effect Emission, 41st AIAA/ASME/SAE/ASEE Joint Propulsion Conference and Exhibit, AIAA, 2005.

39 McLallin, K. "Flywheel Technology Program Overview for NASA MSFC," NASA SRC Power & Propulsion Office Presentation, March 16, 2004.

40 McLallin, K. "Flywheel Technology Program Overview for NASA MSFC," NASA SRC Power & Propulsion Office Presentation, March 16, 2004.

[41] Hoyt, R., Slostad, J., Voronka N., "The Microsatellite Propellantless Electrodynamic Tether (uPET) Propulsion System," 40th Joint Propulsion Conference and Exhibit, AIAA, 2004.

[42] Wertz, J., Larson, W., "Space Mission Analysis and Design," Microcosm Press, 3rd Edition, 1999, Table 17-10, pg. 703.

[43] Hoyt, R., Slostad, J., Twiggs, R., "The Multi-Application Survivable Tether (MAST) Experiment", AIAA-2003-5219, 17th Small Satellite Conference, August 2003, Logan, UT.

44 Stone, N.H., *et al.*, "A Preliminary Assessment of Grid Spheres used as End Body Electrodes for Electrodynamic Tethers," Paper CP608 in *Space Technology and Applications International Forum (STAIF) 2002*.

45 Hoyt, R., Slostad, J., Twiggs, R., "The Multi-Application Survivable Tether (MAST) Experiment", AIAA-2003-5219, 17th Small Satellite Conference, August 2003, Logan, UT.